

1 **Deglaciation of a major palaeo-ice stream in Disko Trough, West Greenland**

2

3 Kelly A. Hogan¹, Colm Ó Cofaigh², Anne E. Jennings³, Julian A. Dowdeswell⁴, John F. Hiemstra⁵

4

5 1 British Antarctic Survey, Natural Environmental Research Council, High Cross, Madingley
6 Road, Cambridge, CB3 0ET, UK7 2 Department of Geography, Durham University, Science Laboratories, South Road, Durham
8 DH1 3LE, UK9 3 INSTAAR and Department of Geological Sciences, University of Colorado, Boulder, Co 80309-
10 0450, USA11 4 Scott Polar Research Institute, University of Cambridge, Lensfield Road, Cambridge, CB2 1ER,
12 UK13 5 Department of Geography, College of Science, Swansea University, Singleton Park, Swansea,
14 SA2 8PP, UK

15

16 **Abstract:** Recent work has confirmed that grounded ice reached the shelf break in central West
17 Greenland during the Last Glacial Maximum (LGM). Here we use a combination of marine
18 sediment-core data, including glacimarine lithofacies and IRD proxy records, and
19 geomorphological and acoustic facies evidence to examine the nature of and controls on the
20 retreat of a major outlet of the western sector of the Greenland Ice Sheet (GrIS) across the shelf.
21 Retreat of this outlet, which contained the ancestral Jakobshavns Isbræ ice stream, from the
22 outer shelf in Disko Trough was rapid and progressed predominantly through iceberg calving,
23 however, minor pauses in retreat (tens of years) occurred on the middle shelf at a trough
24 narrowing forming subtle grounding-zone wedges. By 12.1 cal. kyr BP ice had retreated to a
25 basalt escarpment and shallow banks on the inner continental shelf, where it was pinned and
26 stabilised for at least 100 years. During this time the ice margin appears to have formed a
27 calving bay over the trough and melting became an important mechanism of ice-mass loss. Fine-
28 grained sediments (muds) were deposited alternately with IRD-rich sediments (diamictons)
29 forming a characteristic deglacial lithofacies that may be related to seasonal climatic cycles.
30 High influxes of subglacial meltwater, emanating from the nearby ice margins, deposited muddy
31 sediments during the warmer summer months whereas winters were dominated by iceberg
32 calving leading to the deposition of the diamictons. This is the first example of this glacimarine
33 lithofacies from a continental-shelf setting and we suggest that the calving-bay configuration of
34 the ice margin, plus the switching between calving and melting as ablation mechanisms,

35 facilitated its deposition by channelling meltwater and icebergs through the inner trough. The
36 occurrence of a major stillstand on the inner shelf in Disko Trough demonstrates that the ice-
37 dynamical response to local topography was a crucial control on the behaviour of a major outlet
38 in this sector of the GrIS during retreat.

39

40 **1. INTRODUCTION**

41 During the Last Glacial Maximum (LGM) in Greenland (24-16 ka BP; Funder et al., 2011) ice
42 expanded onto the adjacent continental shelves, although how far the ice sheet extended across
43 the shelf is still a matter of debate in many areas. Based on coastal landforms and, less often,
44 evidence from marine geophysical datasets, ice-sheet reconstructions indicate that the LGM
45 Greenland Ice Sheet (GrIS) was drained at its periphery by a number of confluent ice streams
46 and outlet glaciers (e.g. Evans et al., 2002, 2009; Winkelmann et al., 2010; Roberts and Long,
47 2005; Roberts et al., 2009, 2010, 2013), at least some of which extended to the shelf break in the
48 cross-shelf troughs that dissect the Greenland continental margin (e.g. Dowdeswell et al., 2010,
49 2014; Ó Cofaigh et al., 2013a). These fast-flowing corridors of ice must have been a critical
50 factor affecting the mass balance of the ice sheet, in particular during deglaciation, because they
51 would have dominated the overall discharge in the same way that ice streams and outlet
52 glaciers do for ice sheets today (cf. Bamber et al., 2000; Bennett, 2003). Reconstructing the
53 retreat patterns and chronologies of major marine-terminating outlets since the LGM provides
54 centennial- to millennial-scale records of their behaviour in response to a variety of factors
55 including climatic change and ice-dynamical controls. Improved understanding of these controls
56 is critical in order to increase our ability to predict future responses of the polar ice sheets to
57 ongoing climate change (cf. Velicogna, 2009; Nick et al., 2013). Such palaeo-records also serve as
58 important long-term context for recent and ongoing ice-sheet change, which is occurring today
59 through the thinning and retreat of marine-terminating outlet glaciers and ice streams, in
60 Northwest and Southeast Greenland (Rignot and Kanagaratnam, 2006; Moon et al., 2008; Khan
61 et al., 2010; Velicogna, 2009) and around West Antarctica (Joughin et al., 2003; Rignot et al.,
62 2014).

63 Generating new records of ice retreat from offshore areas in central West Greenland in
64 particular is important for several reasons. Firstly, a large amount of terrestrial
65 geomorphological and deglacial chronological data is available for the Disko Bugt and Sisimiut
66 regions (Weidick, 1972; Kelly, 1985; Funder, 1989); this is because this area is an important
67 drainage route for the modern GrIS via the Jakobshavns Isbræ ice stream, which drains c. 7% of
68 the ice sheet (Joughin et al., 2004). Despite this, information on how the ice sheet was
69 configured on the wide continental shelf in the past, and how and when it deglaciated, is only

70 just emerging (Ó Cofaigh et al., 2013a; Dowdeswell et al., 2014; Jennings et al., 2013;
71 Rinterknecht et al., 2014; Sheldon et al., *this volume*). Furthermore, based on onshore and
72 offshore deglacial chronologies around Greenland it is clear that the final retreat of the GrIS
73 after the LGM was asynchronous, and that it was influenced by both topographic effects and
74 local ice-sheet dynamics, and was not driven solely by climatic change (Bennike and Björck,
75 2002; Funder et al., 2011; Ó Cofaigh et al., 2013a). Identifying and understanding this
76 asynchronicity provides important new information on the behaviour of the GrIS during periods
77 of climatic warming, as well as insights into the dynamic response of ice sheets and their outlets
78 on timescales longer than the observational record.

79 This paper integrates sediment-core data from 10 marine cores with multibeam-bathymetric
80 data and high-resolution acoustic profiles acquired in Disko Trough during cruise JR175 to
81 central West Greenland in 2009. By generating sedimentary lithofacies, IRD proxy, and acoustic
82 facies datasets we determine the style and relative rates of retreat of a major GrIS outlet from its
83 Younger Dryas maximum on the outer shelf, and we examine the importance of local
84 topography on the stability of the outlet's grounded margin during deglaciation. This study also
85 forms part of a wider research agenda to investigate the nature and behaviour of western GrIS
86 ice streams and outlet glaciers over the last glacial-deglacial cycle (Hogan et al., 2011, 2012; Ó
87 Cofaigh et al., 2013a, b; Dowdeswell et al., 2014) and the palaeoenvironmental conditions
88 influencing ice-sheet decay (Lloyd et al., 2005, 2011; Perner et al., 2011; McCarthy, 2011;
89 Jennings et al., 2013; Sheldon et al., *this volume*) from marine geophysical and geological
90 datasets. The work fills an important gap in our knowledge of Greenland's glacial history from
91 offshore areas surrounding the landmass (cf. Funder et al., 2011) and compliments the wealth of
92 terrestrial studies available in the literature (see, for example, Weidick, 1972; Kelly, 1985;
93 Funder, 1989; Bennike and Björck, 2002; Funder and Hansen, 1996, and references therein).

94

95 **1.1. REGIONAL SETTING**

96 Disko Trough is a large bathymetric trough that crosses the continental shelf offshore central
97 West Greenland at around 68° 24'N (Fig. 1). The broad, generally u-shaped cross-profile of the
98 trough is evidence that it has been eroded by glacial ice; however, the trough appears to be
99 fault-bounded on its northern side (Hoffman et al., *this volume*) and most authors believe that
100 successive Quaternary ice advances have followed an older (Pre-Quaternary) drainage system
101 on the shelf (Henderson, 1975; Funder and Larsen, 1989). The trough extends for 195 km from
102 a basalt escarpment on the inner shelf to the outer shelf where there is a small dog-leg diverting
103 the trough axis to the south-west (Fig. 1). Trough width is typically around 40 km but it is
104 variable along its length, with a notable narrowing on the mid-shelf (57° 15'W), east of which

105 the trough widens and deepens; water depths are generally between 400-550 m on the mid-
106 outer shelf. On the inner shelf, the trough is flanked by relatively shallow banks: Disko Banke to
107 the north has typical water depths of 150-250 m, and Store-Hellefiske Banke to the south has
108 water depths of <50 m to 200 m. The shallow banks and escarpment on the inner shelf comprise
109 Palaeogene basalts (Chalmers et al., 1999; Larsen and Pulvertaft, 2000), whereas the
110 continental shelf consists of prograded beds of Late Cretaceous-Quaternary sediments (Rolle,
111 1985; Hoffman et al., *this volume*). East of the basalt escarpment, over which water depths
112 shallow to 300-350 m, is a NNE-SSW trending trough - Egedesminde Dyb - that connects Disko
113 Trough to the Disko Bugt embayment. Taken together, this trough-bay system has a sinuous or
114 “kinked” central axis suggesting that former ice flow of any expanded ice sheet draining through
115 this system may have been strongly affected by topography (cf. Long and Roberts, 2003). At
116 present, water masses on the central West Greenland shelf are dominated by the relatively
117 warm, saline West Greenland Current (WGC), an admixture of the North Atlantic Irminger
118 Current and the East Greenland Current (EGC) (Buch, 1981). The WGC flows northwards over
119 the entire West Greenland shelf, although cold, low-salinity water originating in the EGC,
120 dominates surface waters near the coast (Ribergaard et al., 2008).

121 The traditional view of LGM glaciation in central West Greenland, locally termed the Sisimiut
122 Stade (Kelly, 1985), places the ice-sheet margin at the Fiskebanke moraines which lie on the
123 inner shelf between 10 and 50 km from the coast south of 68°N (Brett and Zarudzki, 1979;
124 Roksandic, 1979). A further set of moraines, the Hellefiske moraines, is found on the outer shelf
125 in southwest Greenland but lies on the middle shelf in central West Greenland (Fig. 1) (Funder
126 and Larsen, 1989). The Hellefiske moraines are usually assigned a Saalian age and the
127 Fiskebanke moraines a Sisimiut age based on correlation of the latter moraines with coastal
128 weathering limits (Kelly, 1985), and extrapolation across the shelf from coastal ice thicknesses
129 (see Funder, 1989; Funder and Hansen, 1996; Funder et al., 2011). However, several studies
130 have since suggested that the LGM margin may instead have extended to the shelf break (e.g.
131 van Tatenhove et al., 1996; Weidick et al., 2004; Roberts et al., 2009), and the compromise view
132 is of a LGM GrIS extending to a limit at the inner shelf moraines with the possibility of ice
133 extending to the shelf break particularly in glacial troughs where increased ice thicknesses and
134 discharge may have promoted ice-stream stability (Long and Roberts, 2002; Roberts et al.,
135 2009). Recent studies from the continental shelf confirm that the GrIS did indeed expand on to
136 the outer shelf in both the Disko and Uummannaq cross-shelf trough systems (Ó Cofaigh et al.,
137 2013a; Dowdeswell et al., 2014). On land, glacially-sculpted landforms suggest that ice in the
138 troughs was fed by confluent ice streams draining into one main outlet on the inner shelf
139 (Roberts and Long, 2005; Roberts et al., 2013); this preferential drawdown of ice into the
140 troughs has been cited as a possible explanation for the widespread evidence of only thin ice at

141 the coastline (Roberts et al., 2013). Ice occupying Disko Trough during the LGM is thought to
142 have been fed by several outlets including the ancestral Jakobshavns Isbræ (ice stream)
143 indicating that the trough was an important drainage route for the GrIS (e.g. Ó Cofaigh et al.,
144 2013; Roberts and Long, 2005; Weidick and Bennike, 2007).

145 Radiocarbon dates from marine-sediment cores provide constraining dates for the
146 withdrawal of ice. Ó Cofaigh et al. (2013) showed that retreat from the shelf break in Disko
147 Trough was well underway by 13.8 cal. kyr BP, but that a short-lived readvance on the outer
148 shelf occurred during the Younger Dryas (YD) and was followed by rapid retreat after 12.2 cal.
149 kyr BP. Using a range of palaeoenvironmental proxy data, Jennings et al. (2013) documented
150 cold oceanographic conditions during retreat from the outer shelf with near permanent sea-ice
151 cover, and no evidence of warm ocean currents entering Disko Trough that may have promoted
152 or enhanced ice decay. Ice-mass loss was predominantly through calving during this rapid
153 retreat phase (Ó Cofaigh et al., 2013a; Jennings et al., 2013). East of the basalt escarpment on
154 the inner shelf, grounded ice had withdrawn from Egedesminde Dyb by 11.1 kyr BP (Kelley et
155 al., 2013), and from eastern Disko Bugt by 10.3 cal. kyr BP (Lloyd et al., 2005) indicating that
156 retreat from the inner shelf to the present-day coastline was much slower than retreat across
157 the continental shelf. At the mouth of Jakobshavns Isfjord the ice margin readvanced or paused
158 around 9.2 kyr BP forming the Marriat moraine system (Young et al., 2011, 2013); offshore the
159 ice margin likely stabilised at a semi-circular submarine bank at the fjord-mouth at this time
160 (Hogan et al., 2012).

161

162 **2. MATERIALS AND METHODS**

163 The data used to reconstruct the style of, and factors influencing deglaciation in Disko Trough
164 consist of 10 marine sediment cores (vibrocores; Table 1), gridded multibeam-bathymetric
165 soundings providing a 3D digital terrain model of the seafloor, and high-resolution acoustic
166 profiles imaging the sub-seafloor sediment units (Fig. 2). These datasets were collected during a
167 NERC-funded research cruise (JR175) of the RSS *James Clark Ross* in August-September, 2009.
168 New chronological information for VC24, VC21, and VC01 is based on calibrated radiocarbon
169 dates; previously published dates from Ó Cofaigh et al. (2013), Jennings et al. (2013) and
170 McCarthy (2011) were also recalibrated in order to be directly comparable to the new dates
171 presented here (see details below).

172 **2.1 Geophysical data**

173 The multibeam-bathymetric data was acquired with a Kongsberg EM120 echosounder
174 operating with a frequency of 12 kHz and emitting 191 across-track beams per ping. The
175 echosounder was run in a 1° by 1° configuration in water depths of between 200 and 600 m in

176 Disko Trough leading to a spatial density of soundings from the seafloor that allowed data to be
177 gridded with cell-sizes of 30-40 m. Bathymetric soundings were processed using a combination
178 of MB-System and Fledermaus software to correct edge artefacts due to the use of poor sound-
179 velocity profiles and to remove spurious data points. High-resolution seismic profiles were
180 acquired concomitantly with the multibeam dataset along the centreline of the swath. These
181 data were collected using a Kongsberg parametric sub-bottom profiler (TOPAS) which has
182 primary frequencies of 15-21 kHz (centred at 18 kHz) and produces a secondary waveform with
183 frequencies between 0.5 and 6 kHz. In the soft seafloor sediments that occur in parts of Disko
184 Trough penetration was up to 50 m below the seafloor; vertical resolution of the data is on the
185 order of a few tens of cm.

186 **2.2 Vibrocores**

187 All vibrocores were acquired using the British geological Survey's corer with a 6-m barrel; core
188 recovery was good with full recovery in soft sediments and penetration of subglacial till in some
189 cores. Lithofacies descriptions and interpretations are based on visual core logs and inspection
190 of x-radiographs of split cores for sedimentary structures including grading, contacts, oversized
191 clast content, deformation structures, bioturbation and the occurrence of mollusc shells. Here
192 we are primarily interested in the deglacial or "transitional" glacial marine units, typically
193 consisting of gravelly-sands or muds with coarse grains or granules, that are often deposited
194 overlying subglacial (diamicton) till facies and stratigraphically below post-glacial (or distal
195 glacial marine) hemipelagic mud facies (cf. Vorren et al., 1984; Domack et al., 2005; Evans et al.,
196 2005). The term diamicton in this paper refers to a poorly sorted admixture of muds, sands and
197 clasts and does not carry an implication for the genesis of this facies, whereas the term till
198 implies a glacial origin to the sediment (cf. Eyles et al., 1983). In the generally fine-grained units
199 above subglacial tills, variations in ice-rafted debris (IRD) (i.e. clasts > 2 mm diameter) are
200 quantified as the number of clasts counted within 2-cm thick by 7-cm wide windows of the x-
201 radiographs (Grobe, 1987). We note that because the x-radiographs are of split cores (rather
202 than 2-cm slabs of sediment) the counts may be somewhat lower than reality as some clasts
203 may be "hidden" behind the thickest sediment in the centre of the core or behind other clasts.
204 Shear strength measurements made every 10 cm using a hand-held torvane are presented for
205 cores VC19-21 and VC23-26. Magnetic susceptibility (MS) data are presented for VC20 and
206 VC24 only, representing a core from the outer and inner parts of Disko Trough, respectively.
207 These physical parameters were measured soon after core splitting at 1-cm intervals on a
208 Geotek Multi-Sensor Core Logger at Durham University. Down-core variations in MS are
209 interpreted to represent changes in the provenance of terrestrial sediments between those with
210 higher contents of magnetic minerals and those with low magnetic mineral contents. In
211 glacial marine settings, MS can also vary with changes in grain size (cf. Kilfeather et al., 2011)

212 whereby larger magnetic particles return higher MS values. On the outer shelf likely sediment
213 sources include Tertiary basalts from the inner shelf (high magnetic mineral contents) and
214 Palaeozoic sedimentary sequences (low magnetic mineral contents) (Jennings et al., 2013;
215 Andrews and Eberl, 2011). One thin section was produced of the basal unit of VC17, allowing
216 the micromorphology of this unit to be analysed.

217 Data for core VC20 including sedimentary lithofacies, IRD counts, shear strength
218 measurements, and radiocarbon dates have been presented by Ó Cofaigh et al. (2013) and
219 Jennings et al. (2013). Here we include only a brief summary of these previously-published data
220 where applicable but we present new MS data for this core and consider the deglacial lithofacies
221 in this core alongside the new results from the other 9 cores.

222 **2.3 Chronology**

223 For new radiocarbon dates from VC24, VC21, and VC01 we apply a ΔR of 140 ± 30 years for
224 Disko Bugt following Lloyd et al. (2011) and Jennings et al. (2013). The dates were calibrated
225 using the online program Calib 7.1 (Stuiver et al., 2015) with the Marine 13.14c calibration
226 curve (Reimer et al., 2013). Although recalibration of the previously-published dates was
227 performed using this most recent software and calibration curve to make sure that the dates
228 were directly comparable, this did not alter the dates when rounded to the nearest 10 years and
229 so the details of the recalibrated dates are not reported here. It is also acknowledged that the
230 local reservoir effect, which is based on information from Disko Bugt - a coastal embayment -
231 may not be appropriate for the middle-outer continental shelf and may have varied during
232 deglaciation around Greenland (cf. Bennike and Björck, 2002). However, this is the best
233 reservoir effect information that we have available at present. Average sedimentation rates
234 were calculated for the lower parts of core VC21 and VC24 using the new dates and existing
235 core chronologies.

236

237 **3. RESULTS AND INTERPRETATION**

238 **3.1 Submarine landforms**

239 **3.2.1 Subtle Transverse Sediment Ridges**

240 *Description:* On the middle shelf in Disko Trough, between about $57^{\circ}30' W$ and $56^{\circ} 25' W$, are
241 several subtle ridges or scarps oriented transverse to the trough axis or slightly oblique to it
242 (Fig. 3). Acoustic profiles show faint sub-bottom reflections beneath the ridges indicating that
243 they comprise wedges of unconsolidated sediments (Fig. 3b). The western ridge (GZW1) is
244 broad and has a subdued and somewhat curved surface profile in cross-section (Fig. 3b); the
245 ridge has a shorter west-facing flank and a longer east-facing flank implying asymmetry.
246 However, both flanks have low average slope gradients around 0.1° with the western slope

247 being slightly steeper (after adjustment by removing the regional seafloor slope). The height of
248 the ridge is around 25 m. Around 56°25' W are two subtle ridges (here termed the central and
249 eastern ridges; GZWs 2 and 3 on Fig. 3) around 10 m in height and oriented NNW-SSE. The
250 central ridge is asymmetrical with a steeper west-facing slope (average slope 0.9°) and a gentler
251 east-facing slope (average 0.3°) whereas the eastern ridge is symmetrical in cross-section. The
252 large western ridge is located at the crest of a landward-deepening section of Disko Trough and
253 the two smaller ridges are situated on this slope (Fig. 3). The two smaller ridges are located
254 around 35 km east of the large ridge and the small ridges are 6 km apart (crest to crest spacing).
255 On sub-bottom profiles the top of the ridges and sedimentary wedges that underlie them are
256 defined by a relatively strong, prolonged reflection with an undulating surface; the wedges
257 comprise acoustically-homogenous to acoustically-transparent material (Fig. 3b). Weak,
258 discontinuous sub-bottom reflections are occasionally visible at depths of several tens of metres
259 below the surface reflection. There are no other units overlying the western wedge (GZW 1) at
260 its shallowest point, but on its east-facing slope is a conformable, homogenous to stratified unit,
261 5-20 m thick that thickens towards the east, i.e. in the overdeepened part of the trough.

262 *Interpretation:* The geometry of the western and central ridges, which are oriented transverse
263 to the axis of the glacial trough, are asymmetric in cross profile with steeper seaward-facing
264 slopes, and are tens of metres thick, have characteristics similar to those of grounding-zone
265 wedges (GZWs) (cf. Ottesen et al., 2005, 2007; Dowdeswell and Fugelli, 2012). GZWs form
266 subglacially at the margins of grounded ice sheets during stillstands in their retreat, which
267 allows for subglacial sediment to build up into a wedge-shaped sediment body along the
268 grounding line (Alley et al., 1986). The ridges in Disko Trough are somewhat different from
269 classic examples of GZWs from the Norwegian-Svalbard (e.g. Ottesen et al., 2005, 2007) and
270 Antarctic continental margins (e.g. Larter and Vanneste, 1995; Anderson, 1999; Ó Cofaigh et al.,
271 2005; Jakobsson et al., 2012) in that they have more subtle morphologies defining only broad
272 ridges rather than distinct seaward-facing scarps (Fig. 6). Moreover, the ridges occur on a
273 landward-dipping slope, which is somewhat unusual for GZWs on northern hemisphere
274 glaciated margins. GZWs most often form at locations where palaeo-ice streams stabilised
275 during retreat, for example, at topographic pinning points including trough constrictions and
276 (or) shallowings (cf. Jamieson et al., 2014).

277 The morphology of the western ridge (GZW1 on Fig. 3), which is very wide in the direction of
278 ice-flow (~35 km) and has low relief (<25 m), does not favour formation as a terminal moraine
279 but it could be an older moraine ridge or GZW that has subsequently been overridden (e.g.
280 Ottesen and Dowdeswell, 2006), although the ridge is wide compared to previously-described
281 overridden moraines. The dimensions and asymmetry of the ridge are more consistent with an

282 interpretation as a GZW. We may explain the subtle and rounded surface expression and the
283 extreme width of this feature as a result of its position on the cusp of a reverse-bed slope. The
284 cusp of the slope would further reduce the already limited accommodation space available for
285 sediment deposition at the grounding zone, assuming that the grounding zone was indeed
286 bounded by an ice shelf and that the wedge of material accumulated in a low-gradient, water-
287 filled cavity beneath the ice shelf (Dowdeswell and Fugelli, 2012). Thus, a relatively thin wedge
288 of subglacial material accumulated over a broad grounding zone, rather than building a
289 pronounced positive relief feature.

290 Our preferred interpretation of the central and eastern ridges in Disko Trough (GZWs 2 and 3
291 on Fig. 3) is as small GZWs deposited during stillstands in the retreat of an ice stream in Disko
292 Trough, although their position on a reverse-bed slope is unusual. Minor GZWs with similar
293 dimensions have recently been identified on the mid-shelf in Uummannaq Trough some 250 km
294 to the north (Dowdeswell et al., 2014). The stratified to homogenous sediment unit overlying
295 the wedges is a deglacial to post-glacial sediment drape deposited from suspension after
296 grounded ice had retreated towards the east. These units correspond to the stratified muds and
297 diamictons and homogeneous muds found in cores VC26 and VC01. Radiocarbon dates from the
298 deglacial sediment units, although not from the area overlying the wedges, are all Holocene in
299 age (Table 2, Jennings et al., 2013) implying that the wedges most likely formed following
300 retreat of ice through the trough from the Younger Dryas extent on the outermost shelf (Ó
301 Cofaigh et al., 2013a).

302 Given that ice-stream retreat was towards the east in Disko Trough, this means that the GZWs
303 identified here occur on a reverse-bed slope. On reverse-bed slopes, in the absence of lateral
304 drag, there is a strong positive feedback that promotes grounding-zone retreat by increasing
305 strain rates and ice losses and destabilizing the grounding-line (Weertman, 1974; Schoof, 2007).
306 However, the regional bathymetry shows that Disko Trough does indeed narrow at the location
307 of GZW1, and, thus lateral drag with the sides of the trough increased in this area and may have
308 temporarily stabilised the ice margin during retreat. GZW1 is also in line (outside of the trough)
309 with the westward extension of the Store-Hellefiske Banke marked by the 200 m contour to the
310 south of the trough, and with a shallow bank (300-350 m deep) on the north side of the trough
311 (Figs. 2, 3). Constriction of the trough width and these bathymetric features likely facilitated any
312 short stillstand(s) during retreat on the mid-shelf.

313

314 **3.2.2 Glacial lineations**

315 *Description:* On the inner shelf there is a small area around 55° 45'W of lineated terrain
316 comprising linear ridges 5-10 m high, several hundred metres wide and extending for between

317 5 and 14 km (limited by the edge of the multibeam data) (Fig. 4a). One broader ridge (about 3
318 km wide) occurs in the deepest part of the trough but disappears to the west. At the eastern end
319 of some of the ridges are streamlined peaks rising around 50 m from the surrounding seafloor.
320 The streamlined peaks and ridges are oriented in an ENE-WSW direction. On TOPAS seismic
321 profiles the upper surfaces of the linear ridges and streamlined peaks are defined by a strong,
322 continuous reflection that is more prolonged on the ridges; rare sub-bottom reflections can be
323 identified beneath the edges of the linear ridges (Fig. 4c). The ridges and peaks are mantled by
324 5-10 m of acoustically-stratified to homogenous material.

325 *Interpretation:* The linear ridges with rounded protuberances at their eastern ends are
326 interpreted as glacial lineations and crag-and-tails (e.g. Hogan et al., 2010; Rydningen et al.,
327 2013) formed subglacially by ice flowing through Disko Trough. The drumlinised protuberances
328 form the “crag” of the crag-and-tail features and confirm that ice flow was from east to west in
329 the trough. The sub-bottom reflections seen on TOPAS profiles beneath the ridges suggest that
330 the “tails” are composed of sediment, whereas the crags probably consist of bedrock (Fig. 4c).

331

332 **3.2.3 Rugged seafloor and channels**

333 *Description:* Between 56° W and 54°30' W the bathymetry in Disko Trough varies sharply
334 between 270 m water depth and 570 m depth (Fig. 4a). The shallow areas are characterised by a
335 rugged morphology that has a N-S to NNE-SSW fabric defined by scalloped to sinuous scarps
336 that are steep on their east-facing sides (3-14°) and dip gently (1-2°) on their western sides. The
337 terrain is smoother in the east and west where rounded crags occur on shallow plateau or
338 mounds and the linear fabric is less defined (Figs. 2, 4a). On the eastern sides of several of the
339 scarps and protuberances are well-defined curvilinear channels that bend around the seafloor
340 highs. Cross-sections of the channels reveal that they are usually u-shaped in profile and can
341 have flat bottoms; maximum widths and depths are around 600 m and 45 m, respectively. In
342 other places the areas between the highs are overdeepened by several tens of metres to form
343 either linear flat-bottomed depressions or linked cavity-depression systems. A second area of
344 rugged seafloor, with scalloped or sinuous scarps up to 20 m high, is present on the outermost
345 shelf (around 58°45' W) in the bathymetry data (Fig. 2); here the escarpments trend NE-SW.
346 Sub-bottom profiles over the rugged seafloor and channels on the inner shelf show that this
347 morphology is defined by a strong, continuous reflection that becomes more diffuse on steep
348 slopes (Fig. 4b); no reflections are visible beneath this impenetrable reflection. The upper
349 reflection is overlain by a 5-20 m thick acoustically-stratified, conformable unit (Figs. 4b, c).

350 *Interpretation:* The sinuous scarps with lineated terrain is easily interpreted as the eroded
351 surface of Palaeogene flood basalts that are known to crop out at the seafloor on the inner shelf

352 in central West Greenland (Chalmers et al., 1998; Bonow, 2005). The escarpments are probably
353 the edges of individual sheet flows, which dip westwards with less than 5° angles in the Disko
354 area (Brett and Zarudzki, 1979; Chalmers et al., 1998) that have presumably been plucked and
355 drumlinised on their eastern sides by glacial ice that flowed over the area from east to west.
356 Faulting may have also contributed to the formation of this rugged terrain (cf. Rydningen et al.,
357 2013). This exposed bedrock is mantled by the conformable sediment unit deposited from
358 suspension after grounded ice had withdrawn from the area. The rugged seafloor on the outer
359 shelf is probably where the multibeam coverage extends over the northern flank of Disko
360 Trough, which has a dog-leg that turns towards the SW on the outer shelf (see Figs. 1, 2). Here
361 the scarps may represent erosion of Quaternary sediments exposed at the seafloor of central
362 West Greenland (Whittaker et al., 1996; Hoffman and Knutz, 2015). Based on seismic-reflection
363 profiles Hoffman and Knutz (2015) have identified two buried palaeo-troughs on the Disko
364 trough-mouth fan (TMF) and hypothesized that these depressions held glacier ice from an
365 earlier glaciation. The recovery of sediments dated to just after the LGM on the southern part of
366 Disko TMF (Ó Cofaigh et al., 2013a, b; Jennings et al., 2013) confirms grounded ice flow through
367 the bathymetric dog-leg to the shelf break during the last glacial.

368 Overdeepenings in the channels, linear depressions and linked cavity-depression systems in the
369 context of this glaciated landscape are indicative of subglacial erosion by meltwater, or a
370 meltwater-sediment mixture. The pressure of the overlying ice allows fluid to flow along
371 gradients in hydraulic potential that are independent of the underlying topography (Shreve,
372 1972) resulting in the formation of overdeepened sections. Thus, the channels and depressions
373 in inner Disko Trough are interpreted as having been eroded by subglacial meltwater and
374 sediment. The timing of their formation is not known although it likely occurred during a period
375 when meltwater was available at the base of the ice sheet, perhaps during deglaciation (cf. Ó
376 Cofaigh et al., 2002). The channels and depressions are similar in appearance and have similar
377 geometries to crescentic scours and sinuous channels around bedrock peaks in other submarine
378 glaciated terrains (e.g. Graham and Hogan, *in press*).

379

380 **3.2 Acoustic facies**

381 Profiles acquired with the TOPAS sub-bottom profiler show that four distinct acoustic facies are
382 present in Disko Trough (Fig. 5). Maximum penetration through the sediment package was 40-
383 50 m. Each of the acoustic facies (AF1- AF4) is described below followed by the interpretation of
384 their depositional setting.

385 *Description:* Acoustic facies 1 (AF1) is found at the seafloor on the outer shelf in Disko Trough
386 and mantling bedrock highs on the inner shelf. It comprises a thin (<10 m) acoustically-

387 homogenous unit that conformably drapes underlying units except on steep slopes where this
388 facies disappears. AF2 is also conformable but it is acoustically-stratified with individual strata
389 being 1-3 m thick (although thinner strata may present but are below the resolution of TOPAS);
390 the total thickness of this unit ranges from 5-20 m. It is present in the deeper E-W trending part
391 of inner Disko Trough (cf. Fig. 5a) and mantling the adjacent rugged basalt highs. AF3 is
392 acoustically homogenous with a moderate to strong, upper reflection that can be prolonged.
393 This unit has variable thickness in Disko Trough tapering to nothing, infilling local depressions
394 (Fig. 5c), and forming positive-relief wedges. Its basal reflection is discontinuous and typically
395 only weak to moderate in strength. AF3 is found at the seafloor on the basalt escarpment where
396 its upper surface is interrupted by iceberg ploughmarks (Fig. 5c). This facies is also found in the
397 subsurface of middle-outer Disko Trough where it is overlain by AF1 and AF2 (Figs. 5b, d);
398 thicknesses range from 0-30 m. The GZWs and glacial lineations (tails of crag-and-tails), which
399 are interpreted as landforms formed subglacially, comprise AF3. AF4 is rare in Disko Trough,
400 occurring only where it infills the E-W deep on the inner shelf (Fig. 5e). It is acoustically
401 transparent and onlaps on to the walls of the depression.

402 *Interpretation:* The conformable geometry of AF1, its position at the top of the acoustic
403 stratigraphy in Disko Trough, and comparison with other glaciated continental shelf settings is
404 consistent with the interpretation of this facies as a post-glacial drape facies deposited by
405 rainout of sediment in a hemipelagic or distal glacimarine setting (e.g. Kleiber et al., 2000;
406 Hogan et al., 2012). The distribution of AF2 is limited to the inner part of Disko Trough and this
407 facies was sampled by cores VC01, VC25, VC23 and VC24. The upper strata of AF2 correspond to
408 the post-glacial massive mud facies in cores VC01 and VC25. In VC23 and VC24, which sampled
409 thinner accumulations of AF2, this stratified facies represents the mud-diamicton units with
410 acoustic reflections between strata presumably corresponding to sub-units with different
411 acoustic properties although it is not possible to correlate specific reflections to core properties
412 with the data available. The mud-diamicton units were interpreted as ice-proximal glacimarine
413 deposits (see Section 3.1.3) and their stratified but conformable nature on sub-bottom profiles
414 is consistent with the deposition of material from suspension (from turbid meltwater plumes)
415 and normal rainout (IRD) processes in glacimarine environments (cf. Hogan et al., 2012). The
416 absence of acoustically-transparent wedges interleaved with stratified reflections suggests that
417 downslope resedimentation was uncommon in inner Disko Trough. Having said this, the
418 occurrence of AF4 in a localised depression only, and its onlapping geometry suggests that this
419 facies consists of material that was focussed into the depression by small-scale slope failures
420 and (or) bottom currents. The unconformable nature of AF3, its varying thickness, and the
421 correlation of this acoustic facies with subglacial landforms (lineations, GZWs) strongly suggest
422 that this acoustic facies represents diamictic material or till deposited in subglacial or proglacial

423 environments (e.g. Ó Cofaigh et al., 2005; Evans et al., 2005). The strong upper reflection of this
424 facies and its acoustically-homogenous character are consistent with the interpretation of AF3
425 as a till, whereby the mixture of grain sizes scatter acoustic energy and the lack of internal
426 structure result in an acoustically-homogeneous response on sub-bottom profiles.

427

428 **3.3 Core lithofacies and sediment accumulation rates**

429 Lithological logs, physical parameter data and IRD counts for cores VC 15, VC17, VC19, VC20,
430 VC21, VC26, VC01, VC25, VC23, and VC24 are presented in Figure 6; example x-radiographs of
431 the lithofacies are given in Figure 7.

432

433 **3.3.1 Facies 1: Diamictons**

434 *Description:* At the base of the cores VC17 and VC19 is a dark grey (5Y 3/1 to 5Y 4/1) stiff
435 diamicton with a muddy matrix supporting a mixture of sand-, gravel- and pebble-sized grains
436 (Fig. 6a). In VC20 the diamicton unit is found between 425 and 520 cm, 19 cm above the base of
437 the core. The diamicton units are generally massive, except for in VC20 where planar
438 discontinuities can be seen on x-radiographs (after Ó Cofaigh et al., 2013a). Contacts with the
439 overlying units are inclined and sharp to relatively sharp in nature. Gravel- and pebble-sized
440 clasts are subangular to subrounded in shape and consist of one of five lithologies: quartzite,
441 granitoid, carbonate, basalt, and a metamorphosed, amphibole-bearing lithology. Clasts are
442 typically 0.3-2 cm in length. Shear-strength measurements from the diamictons range from high
443 (40-80 kPa) in VC20 and VC17 to moderate to low in VC19 (5-15 kPa). A thin section of the
444 diamicton in VC17 at 61-70 cm core-depth reveals sinuous discontinuous cracks in areas of fine-
445 grained matrix and discrete clusters of sand-sized grains or steeply-inclined clasts; turbate
446 structures and shell fragments are rare, and foraminifera are absent. The MS of the diamicton in
447 VC20 is generally low ($20-300 \times 10^{-5}$ SI) and varies from sharp peaks to troughs (Fig. 7).

448 *Interpretation:* On the basis of the high shear strength of the diamicton in VC20, and on the
449 presence of asymmetric deformation structures (parallel fractures, fractured grains turbate
450 structures, lineaments) indicating shear, in a thin section from this unit, Ó Cofaigh et al. (2013)
451 interpreted this diamicton as a subglacial till; this interpretation is maintained here. The
452 variability in the MS probably reflects the changeable grain size of the unit and the fairly low
453 values when compared with overlying units (Fig. 6a) may indicate that the diamicton contains
454 few basaltic clasts because ferromagnetic minerals in basalts retain strong magnetic signatures.
455 The micro-structure of the diamicton in VC17 coupled with its lower shear strength values lead
456 to the interpretation that this unit is a glacial marine diamicton deposited in an ice-proximal
457 setting either as subglacial material emanating from, but deposited in front of, the grounding

458 line, or as an iceberg-rafted deposit. The presence of discrete clusters of grains and deformation
459 at the base of these clusters at the micro-scale indicate an origin as an iceberg-rafted diamicton
460 is most likely; highly inclined to vertical clast orientations observed in the thin section support
461 this interpretation. The low shear strength measurements of the diamicton in VC19 and VC15
462 together with the similarity of these units with the diamicton in VC17 suggests that the VC19
463 and VC15 diamictons can also be interpreted as an iceberg-rafted glacial marine diamictons.

464

465 **3.3.2 Facies 2: Muddy sands with pebbles/muddy sands**

466 *Description:* At the base of VC21 and overlying the diamictons in VC17, VC19, and VC20 are grey-
467 brown (5Y 5/1 to 5Y 5/2), fine to medium, poorly-sorted sand units containing occasional
468 gravel layers and dispersed outsized clasts. Thicknesses of this unit are less than 40 cm in all
469 cores where present; in VC19, our outermost shelf core site, this unit is only 8 cm thick. From
470 visual inspection of the cores the facies appears mostly massive, however x-radiographs reveal
471 that the sands are occasionally weakly- to moderately-laminated to stratified with occasional
472 planar discontinuities (Fig. 8b), and patches of finer-grained material and gravel layers (Fig.
473 8a). In VC21 the unit is moderately-stratified with 2-3 cm thick strata, clast-rich layers and a
474 possible load structure at 486-488 cm core-depth (Fig. 8b). Dispersed or clustered clasts in this
475 unit are subangular to subrounded in shape and are typically between 0.3-1.2 cm in length;
476 quartzite, carbonate, granite, and basalt lithologies occur. The clasts show moderate alignment
477 that is parallel to the planar discontinuities in the core. Counts of clasts >2 mm are moderate to
478 high (4-30 clasts per 2 cm window) but variable in outer shelf cores (VC15, VC17, VC19, VC20);
479 in VC21 the clast content is typically lower (<5 clasts per 2 cm window) (Fig. 8a). Investigations
480 of the microfauna in VC21 indicate that this facies is barren or contains rare, poorly-preserved
481 tests of *Islandiella helenae* and *Cibicides lobatulus*. In VC20 the muddy sands are dominated by *I.*
482 *helenae* but also includes *Cassidulina reniforme* and *Elphidium excavatum* f. *clavata* (Jennings et
483 al., 2013).

484 The shear strength of the muddy sands is moderate with measurements between 10-20 kPa
485 in VC19 and VC20 (Fig. 8a). MS data is only available for VC20 where the values are inconsistent
486 varying between peaks and troughs, and only showing weak correlation with grain size in the
487 unit above the diamicton (Fig. 7a). There, MS values appear to be slightly lower in the coarser-
488 grained facies. In general, MS values appear to be higher in the sands above the diamicton (397-
489 422 cm) than those underlying the diamicton (520-539 cm).

490 *Interpretation:* The up-core transition from diamicton to pebble-rich muddy sands in outer
491 Disko Trough cores (VC15, VC17, VC19, VC20) marks a change in depositional environment
492 from subglacial (VC20) or adjacent to the grounding line (VC17, VC19, VC15) to a location

493 slightly more distal from the ice-stream margin, although still ice proximal. The high clast
494 content and distinct gravel layers and clusters indicate that iceberg rafting was an important
495 process and stratification confirms subaqueous deposition. This unit is interpreted as ice-
496 proximal coarse-grained sediment originating as basal debris from the nearby grounding line
497 (cf. Domack et al., 1999) with additional IRD deposition. The same clast lithologies occur in this
498 facies as were found in the diamictons because both are derived largely from the basal debris
499 zone. The moderate shear strength of Facies 2 reflects compaction and dewatering of this
500 coarse-grained lithofacies by overlying sediments, and the up-core transition from Facies 2 to
501 the overlying fine-grained muds with outsized clasts indicates retreat of the grounding line
502 away from the core sites.

503 The foraminiferal assemblages of the sandy units are an indicator for cold conditions
504 associated with the marginal sea-ice zone (Polyak and Solheim, 1994; Jennings et al., 2013), and
505 for core VC20 Jennings et al. (2013) interpreted this unit to have been deposited during retreat
506 of the ice margin via calving with the setting changing rapidly from ice proximal to ice distal
507 from c. 12.2 to 11.4 cal. kyrs BP. We note that 12.2 cal. kyrs BP is a maximum age for this unit
508 because it is derived from a shell reworked in to this unit from the underlying till and so dates
509 the readvance of ice on to the outer shelf (Ó Cofaigh et al., 2013a). A date of 11.0 cal. kyrs BP
510 from 10 cm above the sandy unit in VC21 (Table 2; Fig. 3a) is consistent with the chronology for
511 retreat in outer Disko Trough but does not further constrain rapid retreat from the outer shelf.

512

513 **3.3.3 Facies 3: Stratified muds and diamictons**

514 *Description:* At the base of cores VC23 and VC24 are thick sequences (up to 200 cm) of stratified
515 grey muds and grey-brown diamictons or sands with outsized clasts, occasional sand lenses,
516 and rare shell fragments (Fig. 6b). The grey sub-units (5Y 5/1 to GLEY 6/1) consist of fine-
517 grained muds with some dispersed clasts; the brown-grey (2.5Y 5/2) sub-units consist of a
518 higher proportion of silt- and sand-sized grains and a high content of dispersed clasts and can
519 be classified as diamictons. The diamicton units are typically thicker (1-3 cm) than the finer-
520 grained units (<1 cm) (Fig. 8c); clasts are largely restricted to the diamicton layers. The clasts
521 are subangular to subrounded and are up to 3 cm in length; clast lithologies are dominantly
522 granite and basalt. Contacts between the coarser- and finer-grained sub-units are horizontal to
523 sub-horizontal, and appear diffuse or gradational on visual inspection of the core. However, x-
524 radiographs of VC24 reveal that the contacts vary from diffuse to sharp (Fig. 8c), and that they
525 are sometimes deformed by load structures or localised faulting. In general, the upper contacts
526 of the diamicton units are sharp whereas their lower contacts are more diffuse or gradational.
527 There is a down-unit trend to better-defined strata with sharper contacts between the sub-

528 units. From 510 cm to the base of the core the finer-grained mud units are laminated and
529 contain coarser 0.1-0.3 cm thick laminae that are sometimes only weakly defined. From 270 cm
530 to 310 cm core depth the unit is bioturbated and vertical burrows have “smeared” or destroyed
531 the mud-diamicton boundaries in patches. In total, there are at least 74 mud-diamicton pairs or
532 “couplets” from 310 cm to the base of the core that can be seen on the x-radiographs.

533 IRD counts from this unit (Fig. 6b) reveal the variable clast content of the mud and diamicton
534 units as distinct peaks and troughs of IRD; 24 distinct IRD peaks can be counted from 310 cm to
535 the base of the core. Slightly increased IRD contents are apparent in the x-radiographs and IRD
536 count data at 490-525 cm core-depth corresponding to higher clast contents in the diamicton
537 sub-units in this interval. Foraminifera tests are rare throughout Facies 3 but some tests of
538 *Cassidulina reniforme* occur in the uppermost 50 cm; *S. biformis*, *S. feylingi* and *E. excavatum*
539 occur between 350 and 400 cm. The MS of the stratified muds varies between about 50 and 200
540 $\times 10^{-5}$ SI (Fig. 7) and is characterised by 66 distinct peaks from 310 cm to the base of the core
541 (above 310 cm this facies is bioturbated).

542 *Interpretation:* The deposition of alternating diamicton and laminated to massive mud units
543 with rare clasts results from switches between glacial marine sedimentation processes during ice
544 retreat in Disko Trough. The diamicton units represent sedimentation predominantly from
545 iceberg rafting, as well as suspension settling of finer grains. The massive to laminated mud
546 facies, however, was deposited when iceberg rafting was overwhelmed by meltwater and fine-
547 grained sediment supply to the trough as is indicated by the very low clast contents. In East
548 Greenland such mud units, when alternating with iceberg-rafted diamictons, have been
549 interpreted as the product of suspension settling during periods with extensive sea-ice cover
550 that prevented iceberg drift over the area (Jennings and Weiner, 1996; Dowdeswell et al., 2000;
551 Smith and Andrews, 2000). In Alaska, such mud-diamicton couplets reflect seasonal switching
552 between sedimentation dominated by settling from turbid meltwater plumes (muds) in summer
553 months and sedimentation from icebergs (diamictons) calved in winter (Cowan et al., 1997; Cai
554 et al., 1997; Ullrich et al., 2009). Although there is some evidence, based on dinocyst proxy data,
555 for near perennial sea-ice cover on the outer shelf in Disko Trough during retreat (Jennings et
556 al., 2013), the occurrence of some large clasts (IRD) in the mud units indicates that icebergs
557 were still passing over the area during the deposition of this facies. In addition, although
558 foraminifera are rare in the stratified unit, the faunal assemblage is associated with modern
559 glacial marine settings (cf. Schafer and Cole, 1986; Jennings and Helgadóttir, 1994), and indicates
560 that turbid meltwater was present during deposition. Thus, we prefer a meltwater origin for the
561 muds with occasional icebergs, over periods of complete sea-ice cover. Facies 3 is interpreted as
562 the product of alternating sedimentation from icebergs and from turbid, subglacially-derived
563 meltwaters with the dominant depositional process varying over time.

564 In the upper part of the mud-diamicton unit in VC24 the diamictons are less well-defined and
565 contain fewer gravel-sized clasts (Fig. 7d) and this is interpreted to represent a gradual increase
566 in the importance of sedimentation from suspension over iceberg calving with time possibly
567 related to ameliorating climatic conditions and, therefore, increased ice-mass loss by melting
568 rather than calving. The occurrence of bioturbation, which becomes extensive towards the top
569 of this unit, also supports ameliorating conditions and retreat of the ice margin further
570 landwards (to the east) during the deposition of these units.

571

572 **3.3.4 Facies 4: Massive to laminated muds**

573 *Description:* The upper 33-455 cm of all of the studied cores in Disko Trough, apart from VC15
574 on the outermost shelf, consists of green-grey to grey massive muds (5Y 4/3 to 5Y 4/1); cores
575 VC01 and VC25 only sampled this unit (Fig. 6b). The muds are heavily bioturbated sometimes
576 with black mottles on their surface, and contain mollusc shells or shelly fragments. They contain
577 only rare outsized clasts and sand-sized grains (Fig. 8e) and are very soft with high water
578 contents; shear-strength measurements are typically less than 5 kPa and free-standing water
579 was present during core logging. MS (based on data from VC01, VC20 and VC24) varies from 10-
580 250×10^{-5} SI with down-core trends varying from increasing (VC20), to decreasing (VC01; not
581 shown) to remaining roughly consistent with multiple peaks and troughs (VC24) (Fig. 7). Noted
582 clast lithologies are carbonates and granites.

583 A full foraminiferal analysis was conducted on VC20 by Jennings et al. (2013) who found that
584 the homogeneous grey-green muds were dominated by agglutinated taxa at their base,
585 including a species indicative of cold conditions and glacial meltwater (*Spiroplectammina*
586 *biformis*), and a cold-water species, *Cuneata arctica*. Calcareous foraminifera, which occur at
587 discrete intervals, were dominated by *Islandiella norcrossi* which is an arctic species indicative
588 of WGC Atlantic water and low amounts of glacial meltwater in Disko Bugt (Lloyd et al., 2005;
589 Perner et al., 2012). At the top of the core warmer water agglutinated forams occur and few
590 carbonate tests suggest poor carbonate preservation in low accumulation rate sediments
591 (Jennings et al., 2013). Evidence from the remaining cores, apart from VC17 which appears to be
592 barren of foraminifera, indicate a similar pattern of agglutinated forams and carbonate tests
593 including *I. helenae*, *Nonionella labradorica*, *E. excavatum* and *C. reniforme* in the lower parts of
594 the muds. Up-core more tests of *I. norcrossi* and *N. labradorica* occur, along with the other Arctic
595 taxa. Radiocarbon dates from the upper 2 m of this facies in VC01 (Table 2) return young ages of
596 less than 2500 cal. yrs BP.

597 *Interpretation:* The homogeneous, bioturbated grey-green muds are interpreted as hemipelagic
598 post-glacial sediments deposited from suspension in an open-marine setting with occasional

599 deposition from icebergs. The post-LGM age of the muds (Jennings et al., 2013) is supported by
600 the new dates from VC01. The foraminiferal assemblages of the muds indicate a transition from
601 cold conditions and the marginal sea-ice zone at their base, to warmer waters and the influence
602 of Atlantic water in the trough. This is consistent with palaeoceanographic records from the
603 inner shelf and Disko Bugt showing that the influence of the WGC only increased after ca. 9.2 ka
604 (Lloyd et al., 2005; McCarthy, 2011). The disappearance of carbonate tests in the uppermost
605 parts of the muds are taken to reflect poor carbonate preservation after Jennings et al. (2013).
606 The presence of carbonate IRD indicates that icebergs from northern Baffin Bay (Andrews and
607 Eberl, 2011) have drifted over Disko Trough during the deposition of this post-glacial mud
608 facies (cf. Jennings et al., 2013).

609

610 **3.1.5 Sediment accumulation rates**

611 The new radiocarbon dates presented here (Table 2) along with previously-published deglacial
612 ages from Disko Trough allow for the calculation of average sedimentation rates for the
613 deglacial lithofacies in VC21 and VC24. Grounded ice retreated from the VC21 core site
614 sometime shortly after 12.24 cal. kyr BP because it is known that ice retreated from VC20 only 6
615 km further west after by this time (Ó Cofaigh et al., 2013a). Consequently, 12.24 cal. kyr BP can
616 be taken as an assumed basal date for VC21. The date of 10.99 cal. kyr BP from 460 cm core-
617 depth in VC21 (Table 2; Fig. 3a) is just above the transition to postglacial muds in the core
618 resulting in an average sedimentation rate for the deglacial unit of 0.04 cm a⁻¹. For VC24, we can
619 use established regional chronology and a tie point with core MSM343340, which is located at
620 the same longitude as VC24 but is 3 km north of the multibeam data coverage (Figs. 2, 4) to
621 constrain the time period during which deglacial sediments accumulated. Ice-retreat from the
622 outer shelf occurred after 12.2 cal kyr BP (O Cofaigh et al., 2013a), and the deepest radiocarbon
623 date in MSM343340 (12.1 cal. kyr BP) has been tied to a depth of 280 cm in VC24, which is near
624 the top of the deglacial sediment unit, by comparing foraminiferal faunas (Perner and Jennings,
625 pers. comm., 2015). Thus, these two dates approximately constrain the age of the stratified,
626 deglacial unit and return an average sedimentation rate for this unit of 2.8 cm a⁻¹. Dates from
627 217-218 cm and 165 cm core-depth in the postglacial mud facies in VC24 (Table 2) give an
628 average sedimentation rate for the lower part of this unit of 0.1 cm a⁻¹.

629

630 **4. DISCUSSION**

631 **4.1 Ice-stream retreat and configuration in Disko Trough**

632 The deglacial lithofacies and IRD counts from vibrocores VC15-VC21 is consistent with rapid
633 ice-stream retreat across the outer shelf after the Younger Dryas readvance to the shelf edge at

634 c. 12.24 cal kyr BP (Ó Cofaigh et al., 2013a; Rinterknecht et al., 2014). The thin, sandy units with
635 abundant IRD (Facies 2) suggest that the cores were located proximal to the ice margin, at one
636 time during overall retreat from the outer shelf, and that the main mechanism for initial ice loss
637 was calving of icebergs. The up-unit decrease in IRD content in these units (Fig. 6a) most likely
638 shows that the ice margin was retreating further eastward during the deposition of these units
639 and, as a result, fewer icebergs passed over the core sites or the majority of the debris had
640 already melted out of the bergs by the time they drifted across the outer shelf. In addition, the
641 thickness of this deglacial facies increases with distance towards land from the shelf break (Fig.
642 6a) suggesting that either retreat was most rapid on the outermost shelf and (or) that
643 winnowing of some sediment occurred. Acoustic profiles confirm that there is very little (<5 m)
644 un lithified sediment cover on the outer shelf over a thin sheet of subglacial till with varying
645 thickness. The till unit, which is sampled in the outer shelf cores (VC15, VC17, VC19, VC20), is
646 evidence for grounded ice flow in Disko Trough during the last glacial but the somewhat
647 surprising absence of any glacial landforms on the outer shelf (cf. Fig.2) may support the
648 inference that the Younger Dryas readvance of grounded ice removed sediments related to ice
649 advance and retreat on the outer shelf during the LGM (Ó Cofaigh et al., 2013a).

650 The rapid initial retreat of ice in Disko Trough over a distance of around 110 km from VC20 to
651 around 55°18'W, which occurred between 12.24 and 12.08 cal. kyr BP (McCarthy, 2011; Ó
652 Cofaigh et al., 2013a) appears to have been punctuated by between 1-3 brief stillstand events
653 during the 160 years of retreat across the shelf (Fig. 9) forming the mid-shelf GZWs (Fig. 3). This
654 tight timeframe is indirect evidence for the rate of formation of GZWs, which must have been
655 built up on the order of decades or less in Disko Trough. The middle ridge in Disko Trough
656 (GZW 2 on Fig. 3), which is most confidently interpreted as a GZW, has an estimated volume of
657 $7.95 \times 10^8 \text{ m}^3$. Assuming that the GZW extends across the entire 20 km-wide trough means that
658 a volume of around $39,750 \text{ m}^3$ per metre of trough width has accumulated during the stillstand
659 event. Estimates of the sediment flux at the grounding line of ice streams in West Antarctica
660 today are on the order of $150 \text{ m}^3 \text{ a}^{-1} \text{ m}^{-1}$ (m^3 per year per metre of ice-stream width)
661 (Anandakrishnan et al., 2007). Using this flux rate the GZW in Disko Trough would have taken
662 265 years to form. Given that marine radiocarbon dates suggest that retreat through this part of
663 the trough occurred in as little as 160 years this flux rate must be too low for the palaeo-ice
664 stream occupying the trough. Supposing that near instantaneous retreat of ice occurred in the
665 trough, and that each GZW (3 total) formed in about 50 years, would require flux rates to be at
666 least five times as high as the modern rates i.e., more than $750 \text{ m}^3 \text{ a}^{-1} \text{ m}^{-1}$. Such large flux rates
667 are not unreasonable; rates on the order of several hundred cubic metres per year per metre ice
668 stream width have been estimated for sediment volumes deposited at the margins of palaeo-ice
669 streams (Dowdeswell et al., 2004) and hypothesized for subglacial till transport at the base of

670 ice streams (Alley et al., 1986; Tulaczyk et al., 2001; Christoffersen et al., 2010). Moreover, a
671 sediment flux as high as $2030 \text{ m}^3 \text{ a}^{-1} \text{ m}^{-1}$ was estimated for the Jakobshavns Isbrae when it was
672 located at the mouth of Jakobshavns Isfjord during deglaciation, with the high flux rate possibly
673 being explained by the narrow geometry ($<10 \text{ km}$) of the fjord (Hogan et al., 2012). However,
674 this discussion again highlights the need for better chronological control on GZWs in order to
675 determine their rates of formation and, thus, their relative significance for ice-stream
676 stabilisation during the retreat of large ice masses. Indeed, the brevity of the YD advance and
677 retreat may suggest that the mid-shelf GZWs were formed during the first retreat of ice from the
678 shelf break, i.e., prior to the YD readvance. However, if correct, these flux rates from the shelf
679 also require relatively thick, grounded ice in Disko Trough during deglaciation in order to
680 deliver this much sediment to the retreating margin. This is somewhat contradictory with
681 modern views on the LGM GrIS which advocate perhaps only thin, lightly grounded outlet
682 glaciers reaching the shelf break in West Greenland (e.g. Roberts et al., 2009, Hoffman et al., *this*
683 *volume*).

684 Once ice had retreated landward of the GZWs in Disko Trough, i.e., east of $56^{\circ}10' \text{ W}$, the
685 deglacial lithofacies (Facies 3, Fig. 8) and acoustic profiles indicate a switch from rapid retreat
686 with ice loss mostly as icebergs to an ice-proximal environment where the release of meltwater
687 became an important mechanism for mass loss. The deepest date in core MSM343340 just north
688 of our multibeam coverage at $55^{\circ}20' \text{ W}$ (Figs. 1, 4) was 12.1 cal. kyr BP (McCarthy, 2011) and
689 confirms that the ice margin was east of the area of rugged seafloor terrain by this time. Indeed,
690 the deglacial stratified mud-diamicton unit (core Facies 3, AF 2) appears to have been deposited
691 rapidly between 12.2 and c. 12.1 cal. kyr BP, at least in VC24 (see Section 3.3.3). The next marine
692 radiocarbon date available is from outer Egedesminde Dyb about 50 km further east and
693 landward of the basalt escarpment that separates Disko Trough from Egedesminde Dyb
694 (Weidick and Bennike, 2007); thus this gives a minimum date for deglaciation to somewhere
695 east of the basalt escarpment by 10.9 cal. kyr BP (Fig. 9) (Quillman et al., 2009). However,
696 terrestrial cosmogenic radionuclide (CRN) exposure ages from Nunarssuaq, an island at the
697 eastern end of Egedesminde Dyb, suggest that the island, and therefore the trough, was
698 deglaciated by 11.1 kyr BP (Kelley et al., 2013). As such, the ice margin may have taken as much
699 as ca. 1000 years (12.1-11.1 kyr BP) to retreat over the basalt plateau and escarpment.

700 Based on the chronology established for the stratified deglacial unit in VC24 (Facies 3, Fig. 8c)
701 these units may have been deposited in as little as 100 years, indicating that stabilisation of the
702 ice on Disko and Store-Hellefiske banks and on the basalt escarpment was probably only for a
703 few hundred years, rather than 1000 years. It is not possible to further constrain the timing of
704 this stillstand from marine data at this time because the existing marine cores do not penetrate
705 the base of the deglacial stratified unit in either Disko Trough or Egedesminde Dyb. However,

706 CRN ages of from the coast just east of Egedesminde Dyb support rapid deposition of the
707 stratified unit as coastal areas were potentially ice-free by 11.9 kyr BP (Kelley et al., 2015; Fig.
708 9).

709 The alternation of diamicton units with laminated muds (core Facies 3, AF2) indicates that,
710 shortly after 12.2 kyr BP, the ice-proximal environment in inner Disko Trough was
711 characterised by periods of iceberg calving and of large influxes of subglacially-derived turbid
712 meltwaters, and that deglacial sediments accumulated over the rugged seafloor terrain (Fig. 4b,
713 c). Assuming that the ice margin was indeed stabilised on the shallow banks and basalt
714 escarpment during this slowdown in retreat, or even on land southeast of Egedesminde Dyb
715 after Kelley et al. (2015), then it seems likely that the inner trough was “surrounded” by
716 grounded ice and that a calving bay (Fig. 10), through which meltwater and icebergs were
717 expelled, existed in inner Disko Trough sometime between c. 12.2 and 11.1 cal kyr BP.
718 Presumably icebergs, meltwater and sediment were channelled primarily through the deep,
719 WNW-ESE trending trough in the southern part of the trough (LGM water depths >480 m; Figs.
720 4a, 9). Indirect support for this comes from sub-bottom profiles showing that the deeper,
721 southern part of the trough contains the thickest deglacial and postglacial sediments (up to 20
722 m of AF1 and AF2) whereas the basalt surfaces are typically mantled with less than 5-8 m of
723 sediment above a thin till unit. However, basin infill and onlapping at the sides of the deep
724 indicates that the redeposition of material from steep sidewalls contributed to the enhanced
725 sediment thicknesses (AF4, Fig. 5e) (cf. Hogan et al., 2012).

726

727 **4.2 Deglacial lithofacies as indicators of style of ice-stream retreat in Disko Trough**

728 The limited thickness of deglacial lithofacies on the outer to middle shelf (Fig. 6a), and their
729 formation as units deposited from the rainout of IRD, indicates that the rapid retreat across the
730 shelf was driven largely by calving rather than melting. Evidence from palaeoenvironmental
731 proxies in VC20 and in cores acquired beyond the shelf break also support rapid ice retreat via
732 calving on the outer shelf (Jennings et al., 2013). It is interesting to note that there does not
733 appear to be a change in the deglacial lithofacies sampled from cores acquired on the outer shelf
734 to VC21 which acquired sediments from immediately seaward of the largest GZW (see Fig. 3a)
735 where the ice margin must have paused, at least for a time, during retreat. We acknowledge,
736 however, that the deglacial lithofacies may be thicker or more variable close to the GZWs than
737 we have described here but that the vibrocorer did not recover these sediments (VC21 bottoms
738 out in an IRD-rich deglacial unit and VC26 contains only post-glacial muds; Fig. 6b).
739 Alternatively, deglacial units from the first retreat from the outer shelf were removed during the
740 YD readvancing ice sheet (cf. Ó Cofaigh et al., 2013a). Thus, we tentatively conclude that the

741 dominant mechanism of ice loss remained the calving of icebergs during this final, rapid retreat
742 phase across the mid-shelf.

743 A major change in the style of retreat, and the mechanisms of ice-mass loss, occurred when
744 the ice margin was located on the inner shelf around 12.2-12.1 cal. kyr BP. At this time ice
745 retreat was punctuated by a major stillstand when the ice margin was likely stabilised on the
746 shallow banks on either side of the trough and on the basalt escarpment at the head of Disko
747 Trough, possibly leading to the formation of a calving bay (see above discussion; Figs. 9, 10).
748 Presumably, the abrupt temperature rise at the start of the Holocene chron at 11.7 ka BP (Dahl-
749 Jensen et al., 1998; Rasmussen et al., 2006) led to high rates of melting and thinning at the ice-
750 sheet margin which increased meltwater and sediment supply to the marine environment. The
751 meltwater flux that resulted from increased temperatures may have been complimented by
752 increased basal melting from the grounded ice margins around the head of the trough as the ice
753 would have had to overcome the shallow, rugged banks in order to drain through the trough. Ice
754 flow over the rough, shallow banks would have caused enhanced basal melting due to increased
755 pressure on the upstream sides of the topographic highs and obstacles at the bed.

756 The deglacial lithofacies (core Facies 3, AF2) from cores acquired on shallower bedrock areas
757 in the trough (VC23-24; Figs. 4a, 9) show that sedimentation from meltwater plumes was a
758 major depositional process at this time and that sedimentation from turbid meltwaters likely
759 overwhelmed the deposition of IRD periodically. The estimate of the average sediment
760 accumulation rate for this unit (2.8 cm a^{-1}) is two orders of magnitude greater than that
761 calculated for the IRD-dominated units on the outer shelf in VC21 (0.04 cm a^{-1}) and VC20 (0.05
762 cm a^{-1} ; Jennings et al., 2013). However, this accumulation rate is much lower than rates of
763 several tens of centimetres per year for mud-diamicton couplets described from Alaskan fjords
764 that are interpreted as strongly seasonal in nature, i.e., glacimarine varves (Cowan et al., 1997;
765 Cai et al., 1997; Ullrich et al., 2009). Using the approximate chronology for the mud-diamicton
766 unit in VC24 (deposited over c. 100 years) and the number of couplets identified in that core
767 from x-radiographs (74) we can calculate an average cyclicity of around 1.3 years for the
768 deposition of each couplet. This is close to being an annual signal especially if we consider that
769 some couplets may be difficult to distinguish visually from x-radiographs if they are particularly
770 thin or absent in colder years with low meltwater basal flux, for example. Therefore, the
771 rhythmicity in the lithofacies could reflect a seasonal response with increased melting in the
772 summer months leading to deposition of fine-grained muds followed by IRD-dominated
773 deposition in winter months when calving is the mode of mass loss. This is similar to the
774 glacimarine varves described from southern Alaskan fjords today, although sedimentation rates
775 are much lower. This probably relates to the difference in climate between temperate Alaskan
776 glacimarine settings which are heavily-influenced by meltwater (cf. Domack and McClennan,

777 1996; Gilbert, 2000) and the subpolar or polar environments on that probably existed in West
778 Greenland during deglaciation, even during the Younger Dryas chron which still had warm
779 summers in southern Greenland (cf. Björck et al., 2002).

780 To our knowledge, this is the first time that stratified, possibly seasonal, mud-diamicton
781 units (core Facies 3) have been described from a continental shelf setting; the examples from
782 Alaska all occur in fjord settings less than 16 km from the calving glacier margin (Cowan et al.,
783 1997). Interestingly, a thin unit (<30 cm) of stratified muds and diamictons also occurs in one
784 core from the inner shelf in Uummannaq Trough (Sheldon et al., *this volume*) about 250 km
785 north of Disko Trough. This suggests that alternating meltwater- and IRD-dominated deposition
786 also occurred in Uummannaq Trough during retreat sometime before 10.8 cal. kyr BP (Sheldon
787 et al., *this volume*). In East Greenland, the stratified mud-diamicton units were found in fjord or
788 fjord-mouth (coastal) environments, where shorefast sea ice could form. Presumably the
789 occurrence of thick (>200 cm) mud-diamicton units on the continental shelf in Disko Trough is
790 related to the confined ice-margin configuration that focussed glacial meltwater and icebergs,
791 and thus deglacial sedimentation, in to inner Disko Trough. This unique ice-margin
792 configuration (i.e. calving bay, Fig. 10) plus an increase in meltwater supply during a stillstand
793 event led to the deposition of the mud-diamicton lithofacies on the inner shelf. In contrast, on
794 the outer shelf retreat occurred primarily by iceberg calving forming the sandy, clast-rich
795 deglacial lithofacies.

796

797 **4.3 Regional Significance**

798 The GZWs in Disko Trough identified here are significant in terms of the regional pattern of
799 ice-sheet retreat in West Greenland. In addition to the GZWs in Disko Trough, large mid-shelf
800 GZWs have also been identified in Uummannaq Trough 250 km to the north (Dowdeswell et al.,
801 2014), and in Fiskanæs Trough 650 km to the south (Ryan et al., *in press*). A bathymetric
802 shallowing that could be a large GZW can also be seen extending across the Holsteinsborg Dyb
803 cross-shelf trough at 66°N in the regional bathymetry (IBCAO v. 3.0; Jakobsson et al., 2012).
804 Similar to Disko Trough, the large GZW in Uummannaq Trough occurs on the cusp of a section of
805 trough with a landward slope but the GZW has a more classic wedge-shaped cross profile (see
806 Fig. 10 in Dowdeswell et al., 2014); in Fiskanæs Trough the GZW, which is several tens of metres
807 high and about 10 km wide, occurs entirely on a reverse-bed slope. The presence of several
808 large GZWs in cross-shelf troughs over a stretch of continental shelf at least 900 km long is
809 perhaps suggestive of a regional ice-sheet stabilisation during deglaciation. Alternatively, it
810 could indicate local topographic effects promoting stabilisation of individual ice streams at
811 different times during retreat. We know from marine dates from Uummannaq Trough and

812 trough-mouth fan (Ó Cofaigh et al., 2013a; Sheldon et al., *this volume*), along with CRN ages and
813 terrestrial geomorphological evidence onshore of Hosteinsborg Dyb (Roberts et al., 2009) that
814 ice extended to the mid-outer shelf in both these troughs during the LGM. In Uummannaq
815 Trough, local topographic effects appear to be limited as the trough is wide (> 50 km) along its
816 length and has a very straight axis, although several bathymetric shallowings do occur on the
817 outer shelf (Sheldon et al., *subm*). Fiskanæs and Holsteinsborg troughs also have straight axes.
818 At present, the detailed chronology of ice-sheet retreat in West Greenland is not known well
819 enough to be able to correlate these glacial landforms over the region but existing dates and
820 reconstructions for the GrIS during deglaciation do not point toward synchronous responses of
821 the ice sheet on the shelf (Ó Cofaigh et al., 2013a; Sheldon et al., *this volume*), although retreat on
822 the inner shelf of West Greenland may have been broadly coherent (e.g. Roberts et al., 2009).

823 The deglaciation of Disko Trough is known to have been somewhat different from retreat in
824 the Uummannaq system. For example, a YD readvance is only known from Disko Trough to
825 date, after which the outlet in this trough retreated across the shelf almost instantaneously. In
826 contrast, ice in Uummannaq Trough likely paused on the mid-shelf for much of the YD (Sheldon
827 et al., *this volume*). Marine dates suggest that ice in Disko Trough was located on the inner shelf
828 (close to the basalt escarpment) by c. 12.2 cal. kyr BP where it may have remained for some
829 time (Fig. 9; Rinterknecht et al., 2014). However, new CRN ages at the coast and on Disko Ejland
830 indicate either that the ice margin was on land, or perhaps more likely, extensive ice-sheet
831 thinning occurred here very shortly afterward (Fig. 9; Kelley et al., 2013, 2015; Rinterknecht et
832 al., 2014). A discussion of the thinning history of the western GrIS is beyond the scope of this
833 paper but the occurrence of deglacial (proximal) facies on the inner shelf being deposited at
834 12.2-12.1 kyr BP confirms that at least the Disko outlet glacier remained in the trough
835 delivering large volumes of sediment and meltwater to Disko Trough even whilst the
836 surrounding ice sheet thinned significantly. At this time the ice margin may have been stabilised
837 on one or both of the shallow banks flanking the trough (Fig. 9). Rinterknecht et al. (2014)
838 explained the residual ice in the trough with concurrent major thinning by suggesting that the
839 outlet glacier had a shallow surface profile beyond the basalt sill, with low basal shear stresses
840 and subglacial meltwater facilitating flow across the shelf. Our landform evidence of meltwater
841 erosion (Fig. 4a, b) and deglacial lithofacies (core Facies 3, AF2) with strong meltwater influence
842 (Fig. 8c) appear to support such a scenario.

843 Despite the fact that the exact timing of margin retreat and the configuration of the margin in
844 and around Disko Trough are not fully known, it is clear that topography was an important
845 control on retreat in this system. The GZWs on the mid-shelf occur in an area where the trough
846 narrows to around 20 km and the banks on the either side of the trough also shallow (Fig. 6). In
847 addition, a more significant stillstand occurred near the head of the trough (this study,

848 Rinterknecht et al., 2014) where shallow banks on either side of the trough and the basalt
849 escarpment likely stabilised retreat (Fig. 9). However, at no point along the wide, straight
850 Ummannaq Trough (cf. Fig. 1) was the flux of ice reduced naturally by a constriction in the
851 trough profile that might have promoted a pause in retreat and GZW formation on the mid-shelf.
852 Indeed, GZW formation there is thought to have been a result of a climatically-induced stillstand
853 during the Bølling-Allerød transition and YD cold periods (Sheldon et al., *this volume*). In
854 contrast, advance and retreat of the Disko outlet occurred during the YD (Ó Cofaigh et al., 2013a;
855 Rinterknecht et al., 2014).

856 Thus, the implication of the new evidence of GrIS retreat presented here is that despite
857 apparent regional similarities in the cross-shelf troughs offshore West Greenland (i.e. middle-
858 shelf GZWs) and periods of rapid retreat via calving, it appears that the pattern of deglaciation
859 in Disko Trough, once initiated, was heavily influenced by local controls on ice dynamics rather
860 than regional climatic or oceanographic effects. In this trough, rapid deglaciation with several
861 very brief pauses and then a more significant stillstand event shows that ice-stream retreat was
862 heavily modulated by local topography around the dog-leg axis and bathymetric pinning points
863 of the trough on the inner shelf. As ice in Disko Trough was stabilised by what must have been
864 grounded ice on the banks we can also become more confident that grounded ice was indeed
865 present on the shallow banks offshore central West Greenland during the LGM (see Fig. 9). This
866 is in contrast to traditional LGM ice-sheet configurations in this area which cite terrestrial
867 hinge-line and geomorphological evidence for ice-free areas on western Disko Ejland and the
868 western part of the Nuussuaq Peninsula (Ingólfsson et al., 1990; Weidick and Bennike, 2007). If
869 these areas were indeed ice free perhaps they existed as nunatuks, or were covered by thin,
870 slow-flowing ice that may have extended to the shelf break (cf. Roberts et al., 2009).
871 Alternatively, confluent fast-ice flow into Disko Trough on the shelf is thought to have been from
872 Jakobsahavns Isbræ (through Disko Bugt) and areas south of the bay (Roberts and Long, 2005)
873 (Fig. 9). Perhaps this ice flux was enough to feed the ice stream in Disko Trough without
874 requiring that the western GrIS overtopped Disko Ejland; a similar drawdown of ice into the
875 Ummannaq Trough from confluent ice streams draining the fjords was put forward by Roberts
876 et al. (2013) to explain ice-free areas and coastal thinning of the ice sheet during deglaciation
877 when marine areas still contained grounded ice. This could explain the discrepancies between
878 marine and terrestrial dates around inner Disko Trough as well (cf. Fig. 9). Certainly, there is
879 good offshore evidence for ice grounding on the Disko Banke up to a latitude of at least 69°30' N
880 in the form of the large Hellefisk moraines (Brett and Zarudzki, 1979) and drainage onto the
881 bank may have been through coastal depressions (see Fig. 1) thus bypassing (and not
882 overtopping) Disko Ejland (Fig. 9).

883 There are still major uncertainties in the LGM ice-sheet configuration for much of central and
884 north Greenland (cf. Funder et al., 2011), and additional discrepancies between the evidence
885 and chronologies available from terrestrial and marine datasets of retreat and thinning
886 histories. Here, we have used new evidence from the marine realm to further our knowledge of
887 deglaciation in a major cross-shelf trough in West Greenland. Recent work shows that ice-
888 stream retreat in Uummannaq Trough appears to have been responsive to climatic forcing and
889 may have been influenced by oceanic warming (Sheldon et al., *this volume*), which is in stark
890 contrast to deglaciation in Disko Trough. Therefore, the factors affecting ice retreat rates during
891 the final deglaciation seem to have been individual to different West Greenland outlets with
892 topographic controls on ice-sheet dynamics and ice-stream dynamics important locally and
893 regional climatic drivers becoming dominant in the absence of significant topographic controls.

894

895 5. CONCLUSIONS

- 896 • Integrated marine geophysical (multibeam bathymetry and acoustic sub-bottom
897 profiles) and geological (sediment cores) datasets from Disko Trough, West Greenland
898 provide new evidence for how a major outlet of the GrIS retreated after the LGM.
899 Lithofacies and radiocarbon dates indicate rapid retreat across the outer and middle
900 shelf that progressed via calving. Retreat was interrupted on the middle shelf by several
901 short-lived (tens of years) stillstands during which sediments built up at the grounded
902 ice margin to form grounding-zone wedges (GZWs). The stillstands occurred at a
903 narrowing of the trough, which reduced the ice flux from the outlet, temporarily
904 stabilising the ice margin.
- 905 • A more major stillstand occurred on the inner shelf when ice was stabilised on a basalt
906 escarpment running across the trough and possibly on the shallow banks (Disko and
907 Store-Hellefiske banks) flanking the trough. Existing deglacial ages from the area show
908 that the stillstand on the inner shelf occurred between ca. 12.2 and 11.1 ka but is
909 unlikely to have lasted for this whole period. The configuration of the ice margin on
910 shallow banks and at the head of the trough likely promoted the formation of a calving
911 bay over inner Disko Trough.
- 912 • During the stillstand periods of high subglacial meltwater influx alternated with times
913 iceberg calving was dominant leading to the deposition of a characteristic mud-
914 diamicton deglacial lithofacies, possibly related to summer-winter climate cycles. This is
915 the first time that this lithofacies has been found on the continental shelf, which is
916 probably a result of the confined ice-margin configuration (calving bay) and high basal
917 melting established during deglaciation.

918 • Advance and retreat of a major West Greenland marine-terminating outlet in Disko
919 Trough occurred during the Younger Dryas cold period. Stillstands during overall
920 retreat occurred at topographic constrictions suggesting that once initiated the
921 dominant controls on retreat in the trough were internal or local factors affecting ice
922 dynamics. Large mid-shelf GZWs exist in cross-shelf troughs over a 900-km long stretch
923 of the West Greenland shelf and are suggestive of a regional response of the GrIS during
924 deglaciation, however, retreat of the Disko Trough outlet was modulated by topography
925 and ice-dynamics rather than climatic or oceanic drivers. This study underlines
926 importance of topographic effects during retreat of major outlets of GrIS in addition to
927 regional drivers, and highlights the need for further deglacial history records from the
928 Greenland continental shelf.

929

930 **Acknowledgements**

931 The data for this study were collected during cruise JR175 of the RSS *James Clark Ross* to West
932 Greenland in 2009 and was funded by Natural Environment Research Council (NERC) grant
933 NE/D001951/1 to C.Ó.C. Funding for this research was also provided by the Unites States
934 National Science Foundation awards: NSF OPP-0713755 and NSF P2C2-1203492 to the
935 University of Colorado. We also thank the officers, crew technical support staff and other
936 scientists on board during JR175 for their assistance with data acquisition. The vibrocorer used
937 on JCR was loaned and operated by staff from the British Geological Survey Marine Operations
938 Group. This work forms part of the British Antarctic Survey program “Polar Science for Planet
939 Earth” funded by the NERC. Lastly, we thank Sam Kelley and one anonymous reviewer for
940 helpful comments on the manuscript.

941

942 **Figure captions:**

943 **Figure 1:** (a) Overview map of Disko Trough and the offshore areas of central West Greenland
944 including major moraines on the shelf and the location of the basalt escarpment at the eastern
945 end of Disko Trough. Also shown is the reconstructed LGM ice margins after Funder et al.
946 (2011) and reconstructed ice-stream margins in Disko and Uummannaq Troughs following
947 recent marine surveying (Ó Cofaigh et al., 2013a; Jennings et al., 2013; Dowdeswell et al., 2014).
948 The imagery over land areas is a 250-m resolution MODIS mosaic produced by Paul Morin using
949 MODIS data from the LANCE (Rapidfire) project
950 (<http://rapidfire.sci.gsfc.nasa.gov/subsets/?mosaic=Arctic>). Some residual snowy areas remain
951 on the south side of Disko Bay and the west side of Disko Ejland. Regional bathymetry is from
952 IBCAO v. 3.0 (Jakobsson et al., 2012). JI: Jakobshavns Isfjord; Eg. Dyb.: Egedesminde Dyb. (b)
953 Seafloor profile over Disko Trough on the mid-shelf, location in (a).

954

955 **Figure 2:** Location of geological (vibrocore) and geophysical (multibeam-bathymetric) datasets
956 in Disko Trough, and previously-reported core locations discussed in the text. SHB: Store-
957 Hellefiske Banke. The locations of subsequent figures are also shown.

958

959 **Figure 3:** (a) Multibeam-bathymetric shaded relief image of subtle sediment wedges
960 interpreted as GZWs on the middle-continental shelf in Disko Trough. The front scarps of the
961 GZWs are delineated with dashed lines and relevant vibrocore locations are shown. (b) TOPAS
962 sub-bottom profile over the GZWs. A faint sub-bottom reflection (arrowed) indicates that the
963 wedges consist of unlithified sedimentary material; for location see (a).

964

965 **Figure 4:** (a) Multibeam-bathymetric shaded relief image of inner Disko Trough showing areas
966 of rugged seafloor with channels (white arrows) landward of basalt scarps, streamlined glacial
967 landforms, the E-W trending deepest part of the trough, and relevant core locations.
968 Bathymetric contour interval is 50 m. The locations of figures 4b, 4c, and the inset are also
969 shown. Inset shows a seafloor profile over MSGL and sedimentary tails of crag-and tails
970 (arrowed) in the inner trough. (b) TOPAS sub-bottom profile over rugged seafloor and the VC24
971 core site. At the seafloor is 5-15 m of acoustically-stratified conformable sediment overlying an
972 impenetrable reflection taken to be the surface of the basalt basement in this area. (c) TOPAS
973 sub-bottom profile over subglacial crag-and-tail landforms indicating ice flow from east to west
974 in the trough. 50 m of acoustically-transparent basin fill occurs in the deepest part of the trough.

975

976 **Figure 5:** Examples of the four acoustic facies (AF1-AF4) observed on TOPAS sub-bottom
977 profiles in Disko Trough. (a) AF1: post-glacial hemipelagic/distal glacimarine drape. (b) AF2:
978 deglacial rainout of suspended sediment and IRD. (c) AF3: subglacial till at the seafloor. (d) AF3:
979 subglacial till facies in the subsurface. (e) AF4: local basin fill. The base of AF3, a faint,
980 discontinuous reflection, is arrowed.

981

982 **Figure 6a:** Sedimentary lithofacies logs, ice-rafted debris (IRD) counts, shear strength (shear
983 str.; for all except VC15), and calibrated AMS radiocarbon dates for cores from outer Disko
984 Trough. Note the different scales on the shear strength plots. Sedimentary logs for VC15 and
985 VC20 and dates marked with an asterisk (*) were reported previously by Ó Cofaigh et al. (2013);

986 IRD counts for VC20 from Jennings et al. (2013). The positions of x-radiographs shown in Figure
987 5 are also shown. Core logs are displayed in order across the West Greenland shelf from the
988 shelf break; see Figure 2 for core locations.

989

990 **Figure 6b:** Sedimentary lithofacies logs, ice-rafted debris (IRD) counts (VC24 only), shear
991 strength (shear str.; for all except VC01), and calibrated AMS radiocarbon dates for cores from
992 inner Disko Trough. Note the different scales on the shear strength plots. The positions of x-
993 radiographs shown in Figure 5 are also shown.

994

995 **Figure 7:** Magnetic susceptibility (MS, SI: International System of Units) for core VC20 on the
996 outer shelf and core VC24 on the inner shelf of Disko Trough.

997

998 **Figure 8:** X-radiographs of sedimentary lithofacies from Disko Trough cores. (a) 18-58 cm core-
999 depth in VC17 showing basal diamicton with diffuse transition to pebble-rich muddy sand and
1000 an change to massive muds at the top of the image. (b) 454-494 cm core-depth in VC21 showing
1001 muddy sands with occasional pebbles, faint wispy laminations (wl), and planar discontinuities
1002 (arrowed). (c) 496-536 cm core-depth in VC24 showing well-defined alternating strata of muds
1003 with rare outsized clasts and diamictons; boundaries between the strata vary from sharp to
1004 diffuse. (d) 291-330 cm core-depth in VC24 showing the upper part of the stratified mud-
1005 diamicton facies with more diffuse boundaries between the strata and bioturbation from 291-
1006 308 cm core-depth. (e) 401-440 cm core-depth in VC21 showing the uppermost lithofacies in
1007 the Disko Trough cores, massive muds with occasional outsized clasts and shells.

1008

1009 **Figure 9:** Reconstruction of ice-margin positions in Disko Trough since the Younger Dryas
1010 readvance to the shelf break based on mapped glacial landforms and dated marine sediments.
1011 Dashed lines indicate conceptual ice-margin positions only. The position of the ice margin
1012 during the stillstand on the inner shelf (black) depicts a calving bay over inner Disko Trough; ice
1013 margin on the banks follows the 200 m contour approximately and connects with the Hellefiske
1014 moraines on the mid-shelf. Outer shelf deglacial ages (calibrated) from Ó Cofaigh et al. (2013),
1015 inner shelf ages from cores MSM343340 and MSM343300 after McCarthy (2011) and Quilman
1016 et al. (2009), respectively; terrestrial radiocarbon age from Long and Roberts (2003).

1017

1018 **Figure 10:** Schematic model of the calving bay in inner Disko Trough during a major stillstand
1019 in ice retreat (not to scale). The ice margin is grounded on the basalt escarpment and shallow
1020 banks flanking the trough; icebergs and meltwater (plumes) are funnelled through the
1021 embayment. Intermittantly sea-ice cover is complete in the leading to the deposition of fine-
1022 grained muds, alternating with periods with reduced sea-ice cover when icebergs can exit the
1023 bay (as drawn) depositing a diamicton deglacial facies.

1024

1025 **Tables:**

1026

Core name	Latitude	Longitude	Water Depth (m)	Length (cm)
VC01	68° 23.9' N	55° 53.9' W	545	270
VC15	67° 54.5' N	58° 43.9' W	347	55
VC17	68° 03.0' N	58° 23.7' W	399	82
VC19	68° 10.5' N	57° 55.7' W	415	204
VC20*	68° 12.1' N	57° 45.4' W	424	539
VC21	68° 13.7' N	57° 37.0' W	430	510
VC23	68° 29.0' N	55° 32.6' W	400	596
VC24	68° 26.9' N	55° 15.2' W	432	563
VC25	68° 22.0' N	55° 47.8' W	521	493
VC26	68° 20.5' N	56° 44.6' W	446	465

1027

1028 **Table 1.** Site information for sediment cores from Disko Trough, West Greenland; core locations
 1029 are shown in Figure 1. *VC20 has been reported previously by Ó Cofaigh et al. (2013) and
 1030 Jennings et al. (2013) and these datasets are cited in the text and figures (see Methods for full
 1031 description of new and previously published data for this core).

1032

Core name	Depth in core (cm)	Carbon source (setting)	Lab. code	¹⁴ C age (B.P.)	1σ min. cal. age - max. cal. age	2σ min. cal. age - max. cal. age	Median calibrated age (cal. yr B.P.)
VC01	24.5	Small shell fragments	CURL-16085	1230 ± 20	624-681	565-716	653
VC01	180-181	Large shell fragments	CURL-16084	2785 ± 20	2290-2394	2207-2415	2332
VC21	460	Paired bivalve shell (<i>Macoma calcarea</i>)	Beta265216	10140 ± 50	10843-11122	10700-11195	10970
VC24	149-150	Single valve, pelecypod	CURL-16082	10525 ± 42	11290-11580	11235-11736	11460
VC24	165	(<i>Yoldiella intermedia</i>)	CURL-16666	10455 ± 42	11208-11393	11174-11615	11320
VC24	217-218	Paired bivalve shell (sp. not known)	CURL-17355	10680 ± 46	11657-11954	11423-12017	11780

1033

1034 **Table 2.** Radiocarbon dates for Disko Trough sediment cores. All dates were calibrated using a
 1035 ΔR of 140 ± 30 following Lloyd et al. (2011), Jennings et al. (2013) and Ó Cofaigh et al. (2013)
 1036 and the calibration program Calib 7.1 with the Marine 13.14c dataset (Reimer et al., 2013).
 1037 Median probability age is rounded to the nearest 10 years.

1038

1039 **References:**

- 1040 Alley, R.B., Blankenship, D.D., Bentley, C.R., Rooney, S.T., 1986. Deformation of till beneath ice
1041 stream B, West Antarctica. *Nature* 322, 57-59.
- 1042 Anandakrishnan, S., Catania, G.A., Alley, R.B., Horgan, H.J., 2007. Discovery of till deposition at
1043 the grounding line of Whillans Ice Stream. *Science* 315, 1835-1838.
- 1044 Andresen, C.S., Kjeldsen, K.K., Harden, B., Nørgaard-Pedersen, N., Kjær, K.H., 2014. Outlet glacier
1045 dynamics and bathymetry at Upernavik Isstrøm and Upernavik Isfjord, North-West Greenland.
1046 *Geological Survey of Denmark and Greenland Bulletin* 31, 79-82.
- 1047 Andrews, J.T., Eberl, D., Scott, D., 2011. Surface (sea floor) and near-surface (box cores)
1048 sediment mineralogy in Baffin Bay as a key to sediment provenance and ice sheet variations.
1049 *Canadian Journal of Earth Sciences* 48, 1307-1328.
- 1050 Bamber, J.L., Vaughan, D.G., Joughin, I., 2000. Widespread Complex Flow in the Interior of the
1051 Antarctic Ice Sheet. *Science* 287, 1248-1250.
- 1052 Bennett, M.R., 2003. Ice streams as the arteries of an ice sheet: their mechanics, stability and
1053 significance. *Earth-Science Reviews* 61, 309-339.
- 1054 Bennike, O., Björck, S., 2002. Chronology of the last recession of the Greenland Ice Sheet. *Journal*
1055 *of Quaternary Science* 17, 211-219.
- 1056 Björck, S., Bennike, O., Rosén, P., Andresen, C.S., Bohncke, S., Kaas, E., Conley, D., 2002.
1057 Anomalously mild Younger Dryas summer conditions in southern Greenland. *Geology* 30, 427-
1058 430.
- 1059 Björck, S., Kromer, B., Johnsen, S., Bennike, O., Hammarlund, D., Lemdahl, G., Possnert, G.,
1060 Rasmussen, T.L., Wohlfarth, B., Hammer, C.U., 1996. Synchronized terrestrial-atmospheric
1061 deglacial records around the North Atlantic. *Science* 274, 1155-1160.
- 1062 Björk, A.A., Kjær, K.H., Korsgaard, N.J., Khan, S.A., Kjeldsen, K.K., Andresen, C.S., Larsen, N.K.,
1063 Funder, S., 2012. An aerial view of 80 years of climate-related glacier fluctuations in southeast
1064 Greenland. *Nature Geoscience* 5, 427-432.
- 1065 Bonow, J.M., 2005. Re-exposed basement landforms in the Disko region, West Greenland—
1066 disregarded data for estimation of glacial erosion and uplift modelling. *Geomorphology* 72, 106-
1067 127.
- 1068 Brett, C.P., Zarudzki, E.F.K., 1979. Project Westmar: a shallow marine geophysical survey on the
1069 West Greenland shelf. *Rapport Grønlands Geologiske Undersøgelse* 87, 1-27.
- 1070 Cai, J., Powell, R.D., Cowan, E.A., Carlson, P.R., 1997. Lithofacies and seismic-reflection
1071 interpretation of temperate glacial marine sedimentation in Tarr Inlet, Glacier Bay, Alaska. *Marine*
1072 *Geology* 143, 5-37.
- 1073 Chalmers, J., Pulvertaft, T., Marcussen, C., Pedersen, A., 1999. New insight into the structure of
1074 the Nuussuaq Basin, central West Greenland. *Marine and Petroleum Geology* 16, 197-224.
- 1075 Christoffersen, P., Tulaczyk, S., Behar, A., 2010. Basal ice sequences in Antarctic ice stream:
1076 exposure of past hydrologic conditions and a principal mode of sediment transfer. *Journal of*
1077 *Geophysical Research: Earth Surface* (2003–2012) 115.

- 1078 Dahl-Jensen, D., Mosegaard, K., Gundestrup, N., Clow, G.D., Johnsen, S.J., Hansen, A.W., Balling, N.,
1079 1998. Past temperatures directly from the Greenland ice sheet. *Science* 282, 268-271.
- 1080 Domack, E., Duran, D., Leventer, A., Ishman, S., Doane, S., McCallum, S., Amblas, D., Ring, J.,
1081 Gilbert, R., Prentice, M., 2005. Stability of the Larsen B ice shelf on the Antarctic Peninsula
1082 during the Holocene epoch. *Nature* 436, 681-685.
- 1083 Domack, E.W., Jacobson, E.A., Shipp, S., Anderson, J.B., 1999. Late Pleistocene–Holocene retreat
1084 of the West Antarctic Ice-Sheet system in the Ross Sea: Part 2—sedimentologic and
1085 stratigraphic signature. *Geological Society of America Bulletin* 111, 1517-1536.
- 1086 Domack, E.W., McClennen, C.E., 2013. Accumulation of Glacial Marine Sediments in Fjords of the
1087 Antarctic Peninsula and their use as Late Holocene Paleoenvironmental Indicators, Foundations
1088 for Ecological Research West of the Antarctic Peninsula. American Geophysical Union, pp. 135-
1089 154.
- 1090 Dowdeswell, J., Cofaigh, C.Ó., Pudsey, C., 2004. Continental slope morphology and sedimentary
1091 processes at the mouth of an Antarctic palaeo-ice stream. *Marine Geology* 204, 203-214.
- 1092 Dowdeswell, J., Fugelli, E., 2012. The seismic architecture and geometry of grounding-zone
1093 wedges formed at the marine margins of past ice sheets. *Geological Society of America Bulletin*
1094 124, 1750-1761.
- 1095 Dowdeswell, J., Ottesen, D., Evans, J., Cofaigh, C.Ó., Anderson, J., 2008. Submarine glacial
1096 landforms and rates of ice-stream collapse. *Geology* 36, 819-822.
- 1097 Dowdeswell, J., Whittington, R., Jennings, A., Andrews, J., Mackensen, A., Marienfeld, P., 2000. An
1098 origin for laminated glacial marine sediments through sea-ice build-up and suppressed iceberg
1099 rafting. *Sedimentology* 47, 557-576.
- 1100 Dowdeswell, J.A., Evans, J., Cofaigh, C.Ó., 2010. Submarine landforms and shallow acoustic
1101 stratigraphy of a 400 km-long fjord-shelf-slope transect, Kangerlussuaq margin, East Greenland.
1102 *Quaternary Science Reviews* 29, 3359-3369.
- 1103 Dowdeswell, J.A., Hogan, K.A., Ó Cofaigh, C., Fugelli, E.M.G., Evans, J., Noormets, R., 2014. Late
1104 Quaternary ice flow in a West Greenland fjord and cross-shelf trough system: submarine
1105 landforms from Rink Isbrae to Uummannaq shelf and slope. *Quaternary Science Reviews* 92,
1106 292-309.
- 1107 Evans, J., Dowdeswell, J.A., Grobe, H., Niessen, F., Stein, R., Hubberten, H.-W., Whittington, R.,
1108 2002. Late Quaternary sedimentation in Keiser Franz Joseph Fjord and the continental margin
1109 of East Greenland. *Geological Society, London, Special Publications* 203, 149-179.
- 1110 Evans, J., Ó Cofaigh, C., Dowdeswell, J.A., Wadhams, P., 2009. Marine geophysical evidence for
1111 former expansion and flow of the Greenland Ice Sheet across the north-east Greenland
1112 continental shelf. *Journal of Quaternary Science*.
- 1113 Evans, J., Pudsey, C.J., Ó Cofaigh, C., Morris, P., Domack, E., 2005. Late Quaternary glacial history,
1114 flow dynamics and sedimentation along the eastern margin of the Antarctic Peninsula Ice Sheet.
1115 *Quaternary Science Reviews* 24, 741-774.
- 1116 Eyles, N., Eyles, C.H., Miall, A.D., 1983. Lithofacies types and vertical profile models; an
1117 alternative approach to the description and environmental interpretation of glacial diamict and
1118 diamictite sequences. *Sedimentology* 30, 393-410.

- 1119 Funder, S., 1989. Quaternary geology of the ice-free areas and adjacent shelves of Greenland, in:
1120 Fulton, R.J. (Ed.), Quaternary Geology of Canada and Greenland. Geological Survey of Canada, pp.
1121 743-792.
- 1122 Funder, S., Hansen, L., 1996. The Greenland ice sheet — a model for its culmination and decay
1123 during and after the last glacial maximum. Bulletin Geological Society of Denmark 42, 137-152.
- 1124 Funder, S., Kjeldsen, K.K., Kjær, K.H., O Cofaigh, C., 2011. The Greenland Ice Sheet During the Past
1125 300,000 Years: A Review, in: Ehlers, J., Gibbard, P., Hughes, P. (Eds.), Quaternary Glaciations -
1126 Extent and Chronology. Part IV: A closer look., pp. 699-713.
- 1127 Funder, S., Larsen, H.C., 1989. Quaternary Geology of the Shelves Adjacent to Greenland, in:
1128 Fulton, R.J. (Ed.), Quaternary Geology of Canada and Greenland. Geological Survey of Canada.
- 1129 Gilbert, R., 2000. Environmental assessment from the sedimentary record of high-latitude
1130 fiords. Geomorphology 32, 295-314.
- 1131 Graham, A.G.C., Hogan, K.A., submitted. Crescentic scours on palaeo-ice stream beds, p. 2.
- 1132 Grobe, H., 1987. A simple method for the determination of ice-rafted debris in sediment cores.
1133 Polarforschung 57, 123-126.
- 1134 Henderson, G., New Bathymetric Maps Covering Offshore West Greenland 59°-69°30'N.
1135 Offshore Technology Conference.
- 1136 Hoffman, J.C., Knutz, P.C., Nielsen, T., Kjuipers, A., *this volume*. Seismic architecture and
1137 evolution of the Disko Bay trough-mouth fan, central West Greenland margin. Submitted to QSR,
1138 PAST Gateways.
- 1139 Hogan, K., Dowdeswell, J., Cofaigh, C.Ó., 2012. Glacimarine sedimentary processes and
1140 depositional environments in an embayment fed by West Greenland ice streams. Marine
1141 Geology 311, 1-16.
- 1142 Hogan, K.A., Dix, J.K., Lloyd, J.M., Long, A.J., Cotterill, C.J., 2011. Seismic stratigraphy records the
1143 deglacial history of Jakobshavn Isbræ, West Greenland. Journal of Quaternary Science 26, 757.
- 1144 Ingólfsson, Ó., Frich, P., Funder, S., Humlum, O., 1990. Paleoclimatic implications of an early
1145 Holocene glacier advance on Disko Island, West Greenland. Boreas 19, 297-311.
- 1146 Jakobsson, M., Anderson, J.B., Nitsche, F.O., Gyllencreutz, R., Kirshner, A.E., Kirchner, N., O'Regan,
1147 M., Mohammad, R., Eriksson, B., 2012. Ice sheet retreat dynamics inferred from glacial
1148 morphology of the central Pine Island Bay Trough, West Antarctica. Quaternary Science Reviews
1149 38, 1-10.
- 1150 Jamieson, S.S., Vieli, A., Cofaigh, C.Ó., Stokes, C.R., Livingstone, S.J., Hillenbrand, C.D., 2014.
1151 Understanding controls on rapid ice-stream retreat during the last deglaciation of Marguerite
1152 Bay, Antarctica, using a numerical model. Journal of Geophysical Research: Earth Surface 119,
1153 247-263.
- 1154 Jennings, A.E., Helgadóttir, G., 1994. Foraminiferal assemblages from the fjords and shelf of
1155 eastern Greenland. Journal of Foraminiferal Research 24, 123-144.
1156
- 1157 Jennings, A.E., Walton, M.E., Ó Cofaigh, C., Kilfeather, A., Andrews, J.T., Ortiz, J.D., De Vernal, A.,
1158 Dowdeswell, J.A., 2014. Paleoenvironments during Younger Dryas-Early Holocene retreat of the

- 1159 Greenland Ice Sheet from outer Disko Trough, central west Greenland. *Journal of Quaternary*
1160 *Science* 29, 27-40.
- 1161 Jennings, A.E., Weiner, N.J., 1996. Environmental change in eastern Greenland during the last
1162 1300 years: evidence from foraminifera and lithofacies in Nansen Fjord, 68 N. *The Holocene* 6,
1163 179-191.
- 1164 Joughin, I., Rignot, E., Rosanova, C.E., Lucchitta, B.K., Bohlander, J., 2003. Timing of recent
1165 accelerations of Pine Island Glacier, Antarctica. *Geophysical Research Letters* 30, 4.
- 1166 Kelley, S.E., Briner, J.P., Young, N.E., 2013. Rapid ice retreat in Disko Bugt supported by 10 Be
1167 dating of the last recession of the western Greenland Ice Sheet. *Quaternary Science Reviews* 82,
1168 13-22.
- 1169 Kelley, S.E., Briner, J.P., Zimmerman, S.R.H., 2015. The influence of ice marginal setting on early
1170 Holocene retreat rates in central West Greenland. *Journal of Quaternary Science*, 30, 271-280.
- 1171 Kelly, M., 1985. A review of the Quaternary geology of western Greenland., in: Andrews, J.T.
1172 (Ed.), *Quaternary environments eastern Canadian Arctic, Baffin Bay, western Greenland*. Allen &
1173 Unwin, Boston, pp. 461-501.
- 1174 Khan, S.A., Wahr, J., Bevis, M., Velicogna, I., Kendrick, E., 2010. Spread of ice mass loss into
1175 northwest Greenland observed by GRACE and GPS. *Geophysical Research Letters* 37.
- 1176 Kilfeather, A.A., Ó Cofaigh, C., Lloyd, J.M., Dowdeswell, J.A., Xu, S., Moreton, S.G., 2011. Ice-stream
1177 retreat and ice-shelf history in Marguerite Trough, Antarctic Peninsula: Sedimentological and
1178 foraminiferal signatures. *Geological Society of America Bulletin*, 123, 997-1015.
- 1179 Larsen, J.G., Pulvertaft, T.C.R., 2000. The structure of the Cretaceous-Palaeogene sedimentary-
1180 volcanic area of Svartehuk Halvø, central West Greenland. *Geological Survey of Denmark and*
1181 *Greenland, Ministry of Environment and Energy*.
- 1182 Larter, R., Vanneste, L., 1995. Relict subglacial deltas on the Antarctic Peninsula outer shelf.
1183 *Geology* 23, 33-36.
- 1184 Lekens, W., Sejrup, H., Hafliðason, H., Petersen, G., Hjelstuen, B., Knorr, G., 2005. Laminated
1185 sediments preceding Heinrich event 1 in the Northern North Sea and Southern Norwegian Sea:
1186 origin, processes and regional linkage. *Marine Geology* 216, 27-50.
- 1187 Lloyd, J.M., Park, L.A., Kuijpers, A., Moros, M., 2005. Early Holocene palaeoceanography and
1188 deglacial chronology of Disko Bugt, West Greenland. *Quaternary Science Reviews* 24, 1741-
1189 1755.
- 1190 Long, A.J., Roberts, D.H., 2002. A revised chronology for the 'Fjord Stade' moraine in Disko Bugt,
1191 west Greenland. *Journal of Quaternary Science* 17, 561-579.
- 1192 Long, A.J., Roberts, D.H., 2003. Late Weichselian deglacial history of Disko Bugt, West Greenland,
1193 and the dynamics of the Jakobshavns Isbrae ice stream. *Boreas* 32, 208-226.
- 1194 McCarthy, D.J., 2011. Late Quaternary ice-ocean interactions in central West Greenland,
1195 Department of Geography. Durham University, p. 292.
- 1196 Moon, T., Joughin, I., 2008. Changes in ice front position on Greenland's outlet glaciers from
1197 1992 to 2007. *Journal of Geophysical Research: Earth Surface* (2003–2012) 113.

- 1198 Nick, F.M., Vieli, A., Andersen, M.L., Joughin, I., Payne, A., Edwards, T.L., Pattyn, F., van de Wal,
1199 R.S., 2013. Future sea-level rise from Greenland/'s main outlet glaciers in a warming climate.
1200 Nature 497, 235-238.
- 1201 Ó Cofaigh, C., Andrews, J., Jennings, A., Dowdeswell, J., Hogan, K., Kilfeather, A., Sheldon, C.,
1202 2013b. Glacimarine lithofacies, provenance and depositional processes on a West Greenland
1203 trough-mouth fan. Journal of Quaternary Science 28, 13-26.
- 1204 Ó Cofaigh, C., Dowdeswell, J.A., Allen, C.S., Hiemstra, J.F., Pudsey, C.J., Evans, J., Evans, D.J., 2005.
1205 Flow dynamics and till genesis associated with a marine-based Antarctic palaeo-ice stream.
1206 Quaternary Science Reviews 24, 709-740.
- 1207 Ó Cofaigh, C., Dowdeswell, J.A., Jennings, A.E., Hogan, K.A., Kilfeather, A.A., Hiemstra, J.F.,
1208 Noormets, R., Evans, J., McCarthy, D.J., Andrews, J.T., Lloyd, J.M., Moros, M., 2013a. An extensive
1209 and dynamic ice sheet on the West Greenland shelf during the last glacial cycle. Geology 41, 219-
1210 222.
- 1211 Ó Cofaigh, C., Pudsey, C.J., Dowdeswell, J.A., Morris, P., 2002. Evolution of subglacial bedforms
1212 along a paleo-ice stream, Antarctic Peninsula continental shelf. Geophysical Research Letters 29,
1213 41-41-41-44.
- 1214 Obbink, E.A., Carlson, A.E., Klinkhammer, G.P., 2010. Eastern North American freshwater
1215 discharge during the Bølling-Allerød warm periods. Geology 38, 171-174.
- 1216 Ottesen, D., Dowdeswell, J., 2006. Assemblages of submarine landforms produced by tidewater
1217 glaciers in Svalbard. Journal of Geophysical Research: Earth Surface (2003–2012) 111.
- 1218 Ottesen, D., Dowdeswell, J., Rise, L., 2005. Submarine landforms and the reconstruction of fast-
1219 flowing ice streams within a large Quaternary ice sheet: The 2500-km-long Norwegian-Svalbard
1220 margin (57–80 N). Geological Society of America Bulletin 117, 1033-1050.
- 1221 Ottesen, D., Dowdeswell, J.A., Landvik, J.Y., Mienert, J., 2007. Dynamics of the Late Weichselian
1222 ice sheet on Svalbard inferred from high-resolution sea-floor morphology. Boreas-International
1223 Journal of Quaternary Research 36, 286-306.
- 1224 Perner, K., Moros, M., Jennings, A., Lloyd, J.M., Knudsen, K.L., 2012. Holocene palaeoceanographic
1225 evolution off West Greenland. The Holocene, 0959683612460785.
- 1226 Perner, K., Moros, M., Lloyd, J., Kuijpers, A., Telford, R., Harff, J., 2011. Centennial scale benthic
1227 foraminiferal record of late Holocene oceanographic variability in Disko Bugt, West Greenland.
1228 Quaternary science reviews 30, 2815-2826.
- 1229 Polyak, L., Solheim, A., 1994. Late-and postglacial environments in the northern Barents Sea
1230 west of Franz Josef Land. Polar Research 13, 197-207.
- 1231 Quillmann, U., Jennings, A.E., Bendle, J., Jonsdóttir, H., Kristjansdóttir, G.B., Lloyd, J., Ólafsdóttir,
1232 S., Principato, S., 2009. Radiocarbon Date List XI: Radiocarbon Dates from Marine Sediment
1233 Cores of the Iceland, Greenland, and Northeast Canadian Arctic Shelves and Nares Strait.
1234 Occasional Paper - Colorado University, Institute of Arctic and Alpine Research 59, 69.
- 1235 Rasmussen, S.O., Andersen, K.K., Svensson, A., Steffensen, J.P., Vinther, B.M., Clausen, H.B.,
1236 Siggaard-Andersen, M.L., Johnsen, S.J., Larsen, L.B., Dahl-Jensen, D., 2006. A new Greenland ice
1237 core chronology for the last glacial termination. Journal of Geophysical Research: Atmospheres
1238 (1984–2012) 111.

- 1239 Reimer, P.J., Bard, E., Bayliss, A., Beck, J.W., Blackwell, P.G., Bronk Ramsey, C., Buck, C.E., Cheng,
1240 H., Edwards, R.L., Friedrich, M., 2013. IntCal13 and Marine13 radiocarbon age calibration curves
1241 0-50,000 years cal BP.
- 1242 Rignot, E., Kanagaratnam, P., 2006. Changes in the Velocity Structure of the Greenland Ice Sheet.
1243 Science 311, 986-990.
- 1244 Rignot, E., Mouginot, J., Morlighem, M., Seroussi, H., Scheuchl, B., 2014. Widespread, rapid
1245 grounding line retreat of Pine Island, Thwaites, Smith, and Kohler glaciers, West Antarctica,
1246 from 1992 to 2011. Geophysical Research Letters 41, 3502-3509.
- 1247 Rinterknecht, V., Jomelli, V., Brunstein, D., Favier, V., Masson-Delmotte, V., Bourlès, D., Leanni, L.,
1248 Schläppy, R., 2014. Unstable ice stream in Greenland during the Younger Dryas cold event.
1249 Geology 42, 759-762.
- 1250 Roberts, D.H., Long, A.J., 2005. Streamlined bedrock terrain and fast ice flow, Jakobshavns
1251 Isbrae, West Greenland: implications for ice stream and ice sheet dynamics. Boreas 34, 25-42.
- 1252 Roberts, D.H., Long, A.J., Davies, B.J., Simpson, M.J., Schnabel, C., 2010. Ice stream influence on
1253 West Greenland ice sheet dynamics during the Last Glacial Maximum. Journal of Quaternary
1254 Science 25, 850-864.
- 1255 Roberts, D.H., Rea, B.R., Lane, T.P., Schnabel, C., Rodés, A., 2013. New constraints on Greenland
1256 ice sheet dynamics during the last glacial cycle: evidence from the Uummannaq ice stream
1257 system. Journal of Geophysical Research: Earth Surface 118, 519-541.
- 1258 Roberts, D.H., Long, A.J., Lloyd, J.M., Schnabel, C., Davies, B.J., Xu, S., Simpson, M.J.R., Huybrechts,
1259 P., 2009. Ice sheet extent and early deglacial history of the southwestern sector of the Greenland
1260 Ice Sheet. Quaternary Science Reviews 28, 2760-2773.
- 1261 Roksandic, M.M., 1979. Geology of the continental shelf off West Greenland between 61°15'N
1262 and 64°00'N. Grønlands geologiske Undersøgelse 92, 15.
- 1263 Rolle, F., 1985. Late Cretaceous-Tertiary sediments offshore central West Greenland:
1264 lithostratigraphy, sedimentary evolution, and petroleum potential. Canadian Journal of Earth
1265 Sciences 22, 1001-1019.
- 1266 Ryan, J.C., Dowdeswell, J.A., Hogan, K.A., accepted. Three cross-shelf troughs on the continental
1267 shelf of Southwest Greenland from Olex data. in: Dowdeswell, J.A., Canals, M., Todd, B.J.,
1268 Jakobsson, M., Dowdeswell, E.K., Hogan, K.A. (Eds.), The Atlas of Submarine Glacial Landforms,
1269 Geological Society of London Memoir Series.
- 1270 Rydningen, T. A., Vorren, T. O., Laberg, J. S., Kolstad, V., 2013. The marine-based Fennoscandian
1271 Ice Sheet: glacial and deglacial dynamics as reconstructed from submarine landforms.
1272 Quaternary Science Reviews 68, 126-141.
- 1273 Schoof, C., 2007. Ice sheet grounding line dynamics: Steady states, stability, and hysteresis.
1274 Journal of Geophysical Research: Earth Surface (2003–2012) 112.
- 1275 Sheldon, C., Jennings, A.E., Andrews, J.T., Ó Cofaigh, C., Hogan, K.A., Seidenkrantz, M.-S.,
1276 Dowdeswell, J.A., submitted. Ice Stream retreat following the LGM and development onset of the
1277 West Greenland Current in the Uummannaq Trough System, West Greenland.
- 1278 Schafer, C.T., Cole, F.E., 1986. Reconnaissance survey of benthonic foraminifera from Baffin
1279 Island fiord environments. Arctic 39, 232-239.

- 1280 Shreve, R., 1972. Movement of water in glaciers. *Journal of Glaciology* 11, 205-214.
- 1281 Smith, L.M., Andrews, J.T., 2000. Sediment characteristics in iceberg dominated fjords,
1282 Kangerlussuaq region, East Greenland. *Sedimentary Geology* 130, 11-25.
- 1283 Steffensen, J.P., Andersen, K.K., Bigler, M., Clausen, H.B., Dahl-Jensen, D., Fischer, H., Goto-Azuma,
1284 K., Hansson, M., Johnsen, S.J., Jouzel, J., Masson-Delmotte, V., Popp, T., Rasmussen, S.O.,
1285 Röthlisberger, R., Ruth, U., Stauffer, B., Siggaard-Andersen, M.-L., Sveinbjörnsdóttir, Á.E.,
1286 Svensson, A., White, J.W.C., 2008. High-Resolution Greenland Ice Core Data Show Abrupt Climate
1287 Change Happens in Few Years. *Science* 321, 680-684.
- 1288 Stuiver, M., Reimer, P.J., Reimer, R.W., 2015. CALIB 7.1. Available online at: calib.qub.ac.uk/calib.
- 1289 Tulaczyk, S.M., Scherer, R.P., Clark, C.D., 2001. A ploughing model for the origin of weak tills
1290 beneath ice streams: a qualitative treatment. *Quaternary International* 86, 59-70.
- 1291 Ullrich, A.D., Cowan, E.A., Zellers, S.D., Jaeger, J.M., Powell, R.D., 2009. Intra-annual variability in
1292 benthic foraminiferal abundance in sediments of Disenchantment Bay, an Alaskan glacial fjord.
1293 *Arctic, Antarctic, and Alpine Research* 41, 257-271.
- 1294 van Tatenhove, F.G., van der Meer, J.J., Koster, E.A., 1996. Implications for deglaciation
1295 chronology from new AMS age determinations in central West Greenland. *Quaternary Research*
1296 45, 245-253.
- 1297 Velicogna, I., 2009. Increasing rates of ice mass loss from the Greenland and Antarctic ice sheets
1298 revealed by GRACE. *Geophysical Research Letters* 36.
- 1299 Vorren, T. O., Hald, M., Thomsen, E., 1984. Quaternary sediments and environments on the
1300 continental shelf off northern Norway. *Marine Geology* 57, 229-257.
- 1301 Weertman, J., 1974. Stability of the junction of an ice sheet and an ice shelf. *Journal of Glaciology*
1302 13, 3-11.
- 1303 Weidick, A., 1972. Holocene shore-lines and glacial stages in Greenland – an attempt at
1304 correlation. *Rapport Grønlands Geologiske Undersøgelse* 41, 39.
- 1305 Weidick, A., Bennike, O., 2007. Quaternary glaciation history and glaciology of Jakobshavn Isbræ
1306 and the Disko Bugt region, West Greenland: a review. *Geological Survey of Denmark and*
1307 *Greenland*.
- 1308 Weidick, A., Kelly, M., Bennike, O., 2004. Late Quaternary development of the southern sector of
1309 the Greenland Ice Sheet, with particular reference to the Qassimiut lobe. *Boreas-International*
1310 *Journal of Quaternary Research* 33, 284-299.
- 1311 Winkelmann, D., Jokat, W., Jensen, L., Schenke, H.W., 2010. Submarine end moraines on the
1312 continental shelf off NE Greenland - Implications for Lateglacial dynamics. *Quaternary Science*
1313 *Reviews* 29, 1069-1077.
- 1314 Young, N.E., Briner, J.P., Axford, Y., Csatho, B., Babonis, G.S., Rood, D.H., Finkely, R.C., 2011.
1315 Response of a marine terminating Greenland outlet glacier to abrupt cooling 8200 and 9300
1316 years ago. *Geophysical Research Letters* 38, L24701.
- 1317 Young, N.E., Briner, J.P., Rood, D.H., Finkel, R., C., Corbett, L.B., Bierman, R., 2013. Age of the Fjord
1318 Stade moraines in the Disko Bugt region, western Greenland, and the 9.3 and 8.2 ka cooling
1319 events. *Quaternary Science Reviews* 60, 76–90.

Tables:

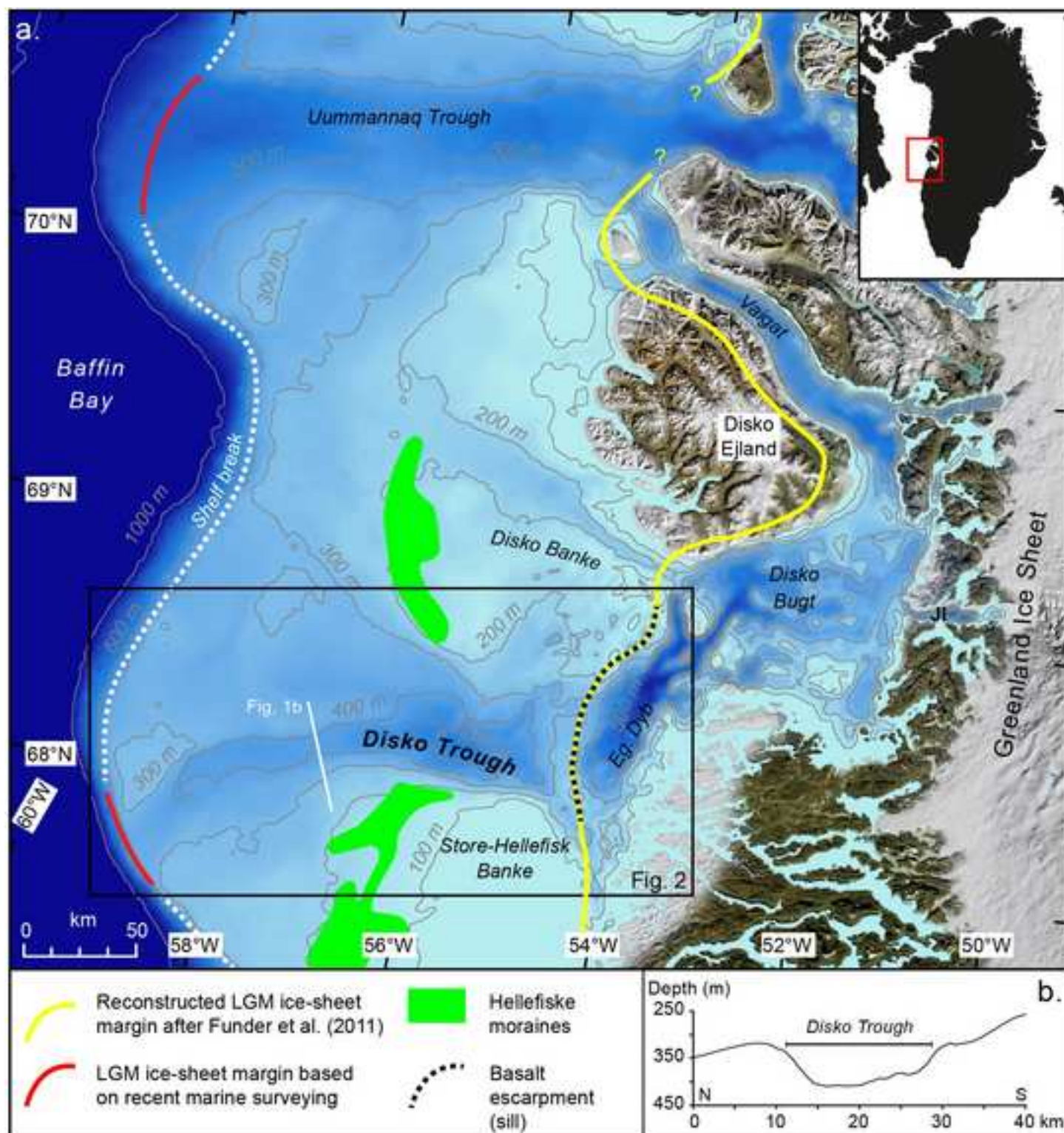
Core name	Latitude	Longitude	Water Depth (m)	Length (cm)
VC01	68° 23.9' N	55° 53.9' W	545	270
VC15	67° 54.5' N	58° 43.9' W	347	55
VC17	68° 03.0' N	58° 23.7' W	399	82
VC19	68° 10.5' N	57° 55.7' W	415	204
VC20*	68° 12.1' N	57° 45.4' W	424	539
VC21	68° 13.7' N	57° 37.0' W	430	510
VC23	68° 29.0' N	55° 32.6' W	400	596
VC24	68° 26.9' N	55° 15.2' W	432	563
VC25	68° 22.0' N	55° 47.8' W	521	493
VC26	68° 20.5' N	56° 44.6' W	446	465

Table 1. Site information for sediment cores from Disko Trough, West Greenland; core locations are shown in Figure 1. *VC20 has been reported previously by Ó Cofaigh et al. (2013) and Jennings et al. (2013) and these datasets are cited in the text and figures (see Methods for full description of new and previously published data for this core).

Core name	Depth in core (cm)	Carbon source (setting)	Lab. code	¹⁴ C age (B.P.)	1σ min. cal. age - max. cal. age	2σ min. cal. age - max. cal. age	Median calibrated age (cal. yr B.P.)
VC01	24.5	Small shell fragments	CURL-16085	1230 ± 20	624-681	565-716	653
VC01	180-181	Large shell fragments	CURL-16084	2785 ± 20	2290-2394	2207-2415	2332
VC21	460	Paired bivalve shell (<i>Macoma calcarea</i>)	Beta265216	10140 ± 50	10843-11122	10700-11195	10970
VC24	149-150	Single valve, pelecypod	CURL-16082	10525 ± 42	11290-11580	11235-11736	11460
VC24	165	(<i>Yoldiella intermedia</i>)	CURL-16666	10455 ± 42	11208-11393	11174-11615	11320
VC24	217-218	Paired bivalve shell (sp. not known)	CURL-17355	10680 ± 46	11657-11954	11423-12017	11780

Table 2. Radiocarbon dates for Disko Trough sediment cores. All dates were calibrated using a ΔR of 140 ± 30 following Lloyd et al. (2011), Jennings et al. (2013) and Ó Cofaigh et al. (2013) and the calibration program Calib 7.1 with the Marine 13.14c dataset (Reimer et al., 2013). Median probability age is rounded to the nearest 10 years.

Figure 1
[Click here to download high resolution image](#)



Figure

[Click here to download high resolution image](#)

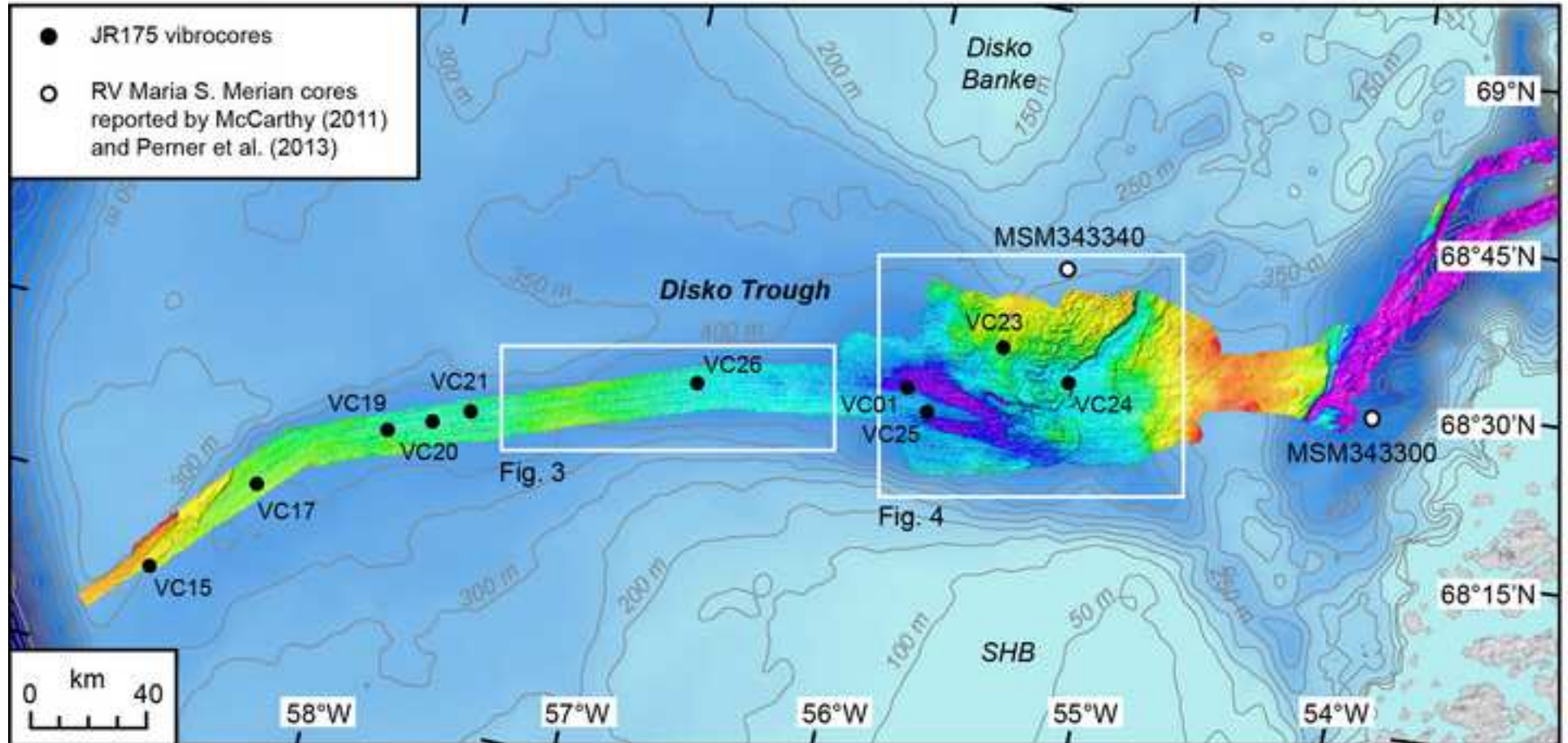


Figure 3
[Click here to download high resolution image](#)

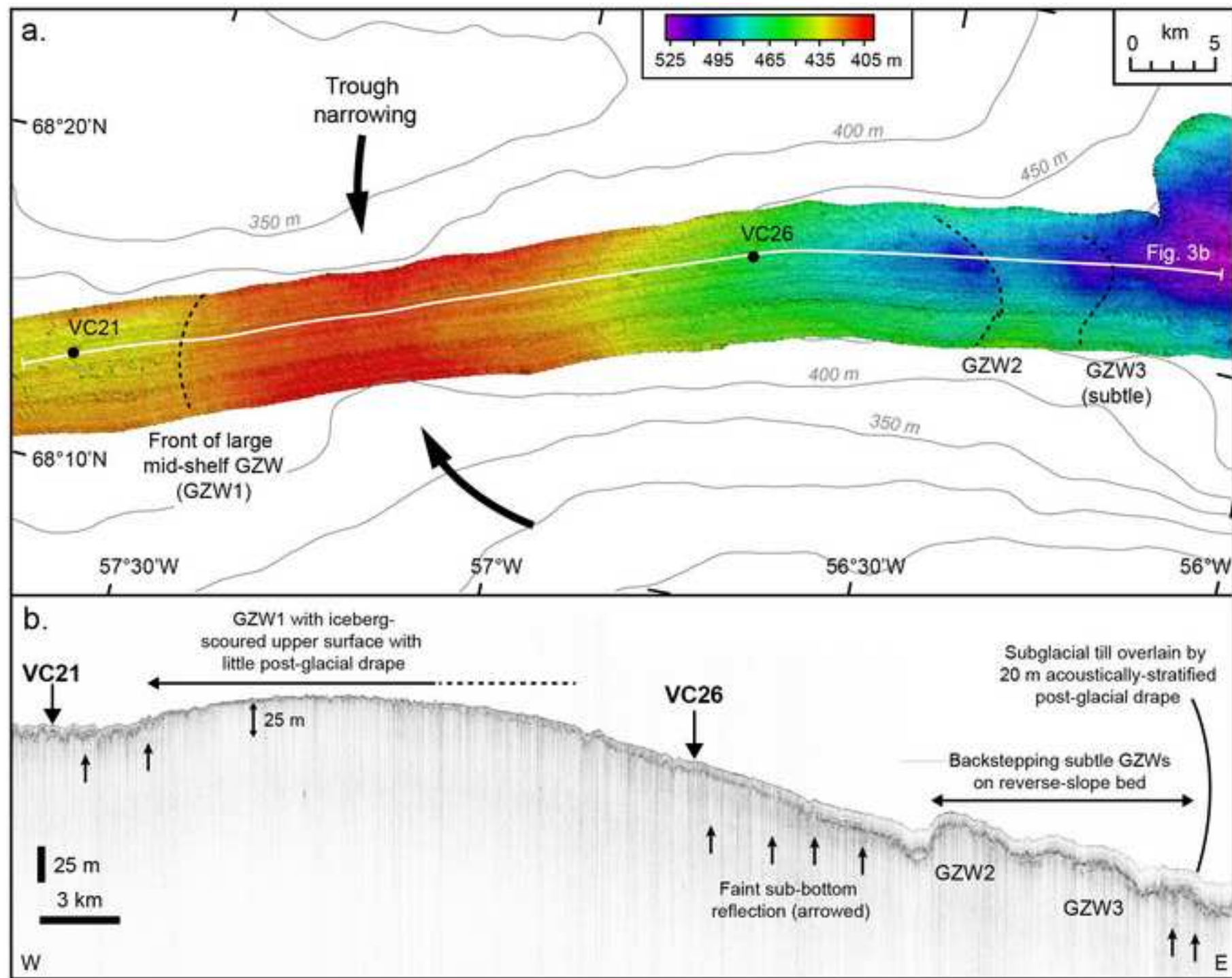
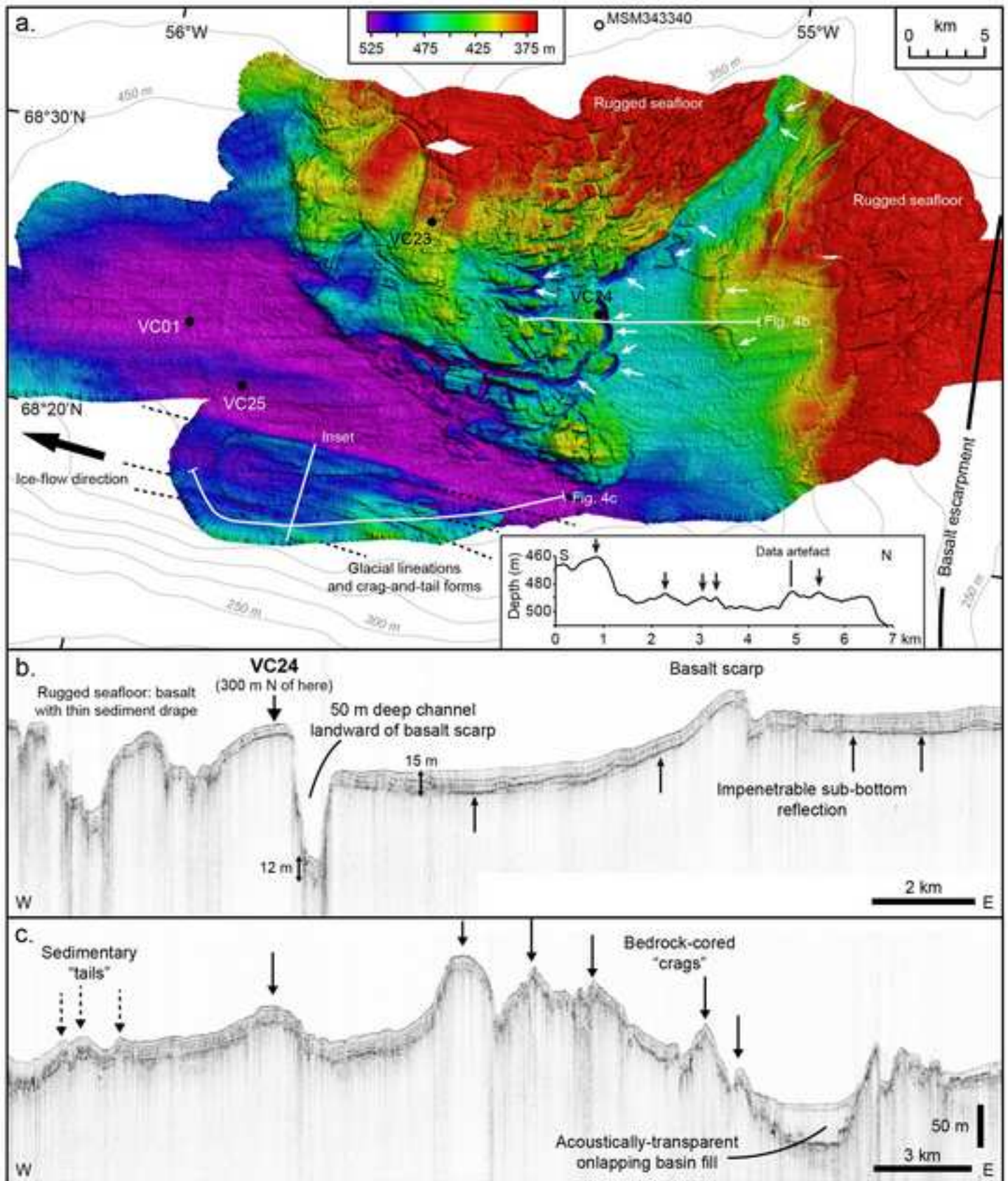


Figure 4
[Click here to download high resolution image](#)



Figure

[Click here to download high resolution image](#)

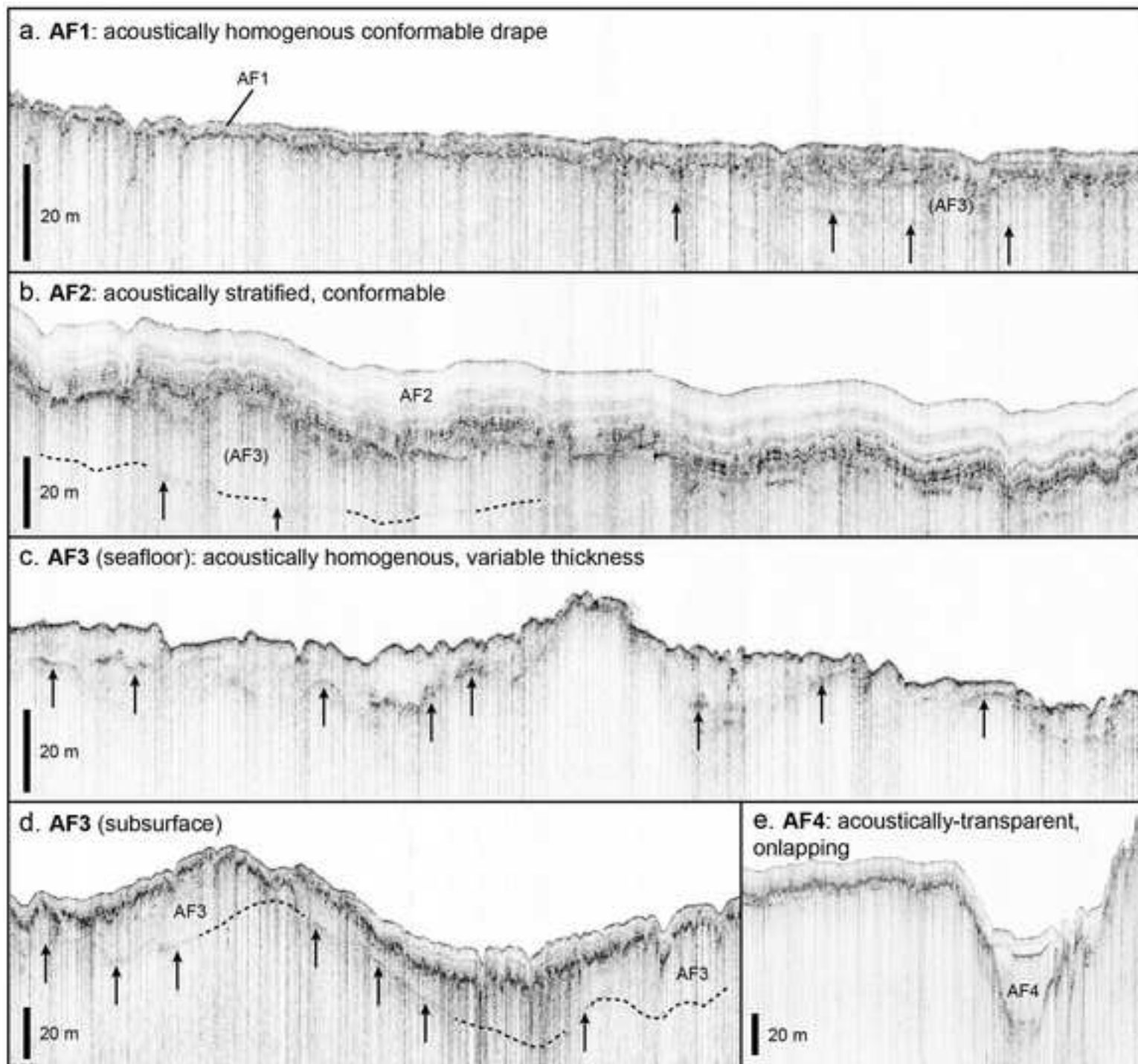


Figure 6a

[Click here to download high resolution image](#)

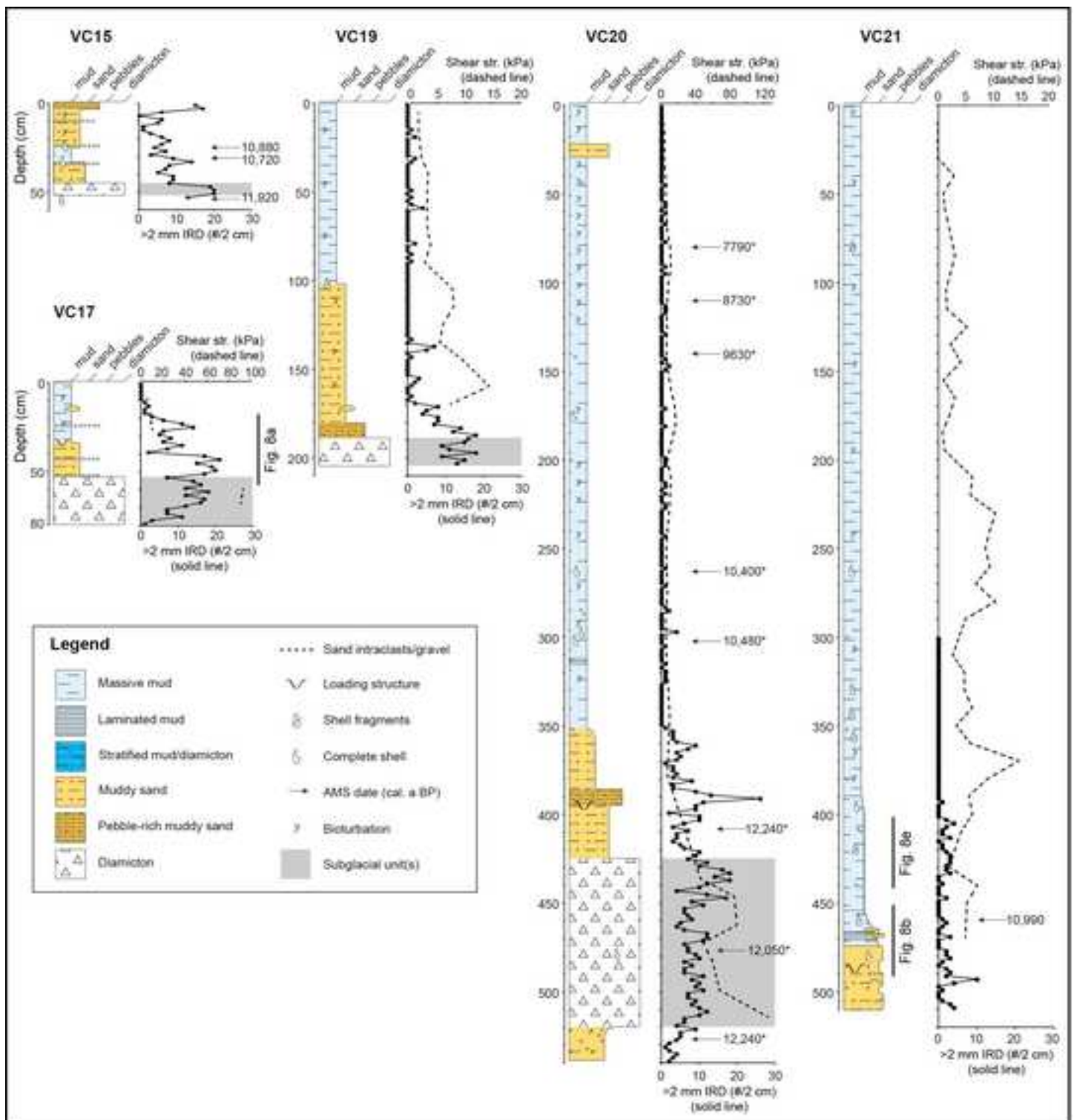


Figure 6b
[Click here to download high resolution image](#)

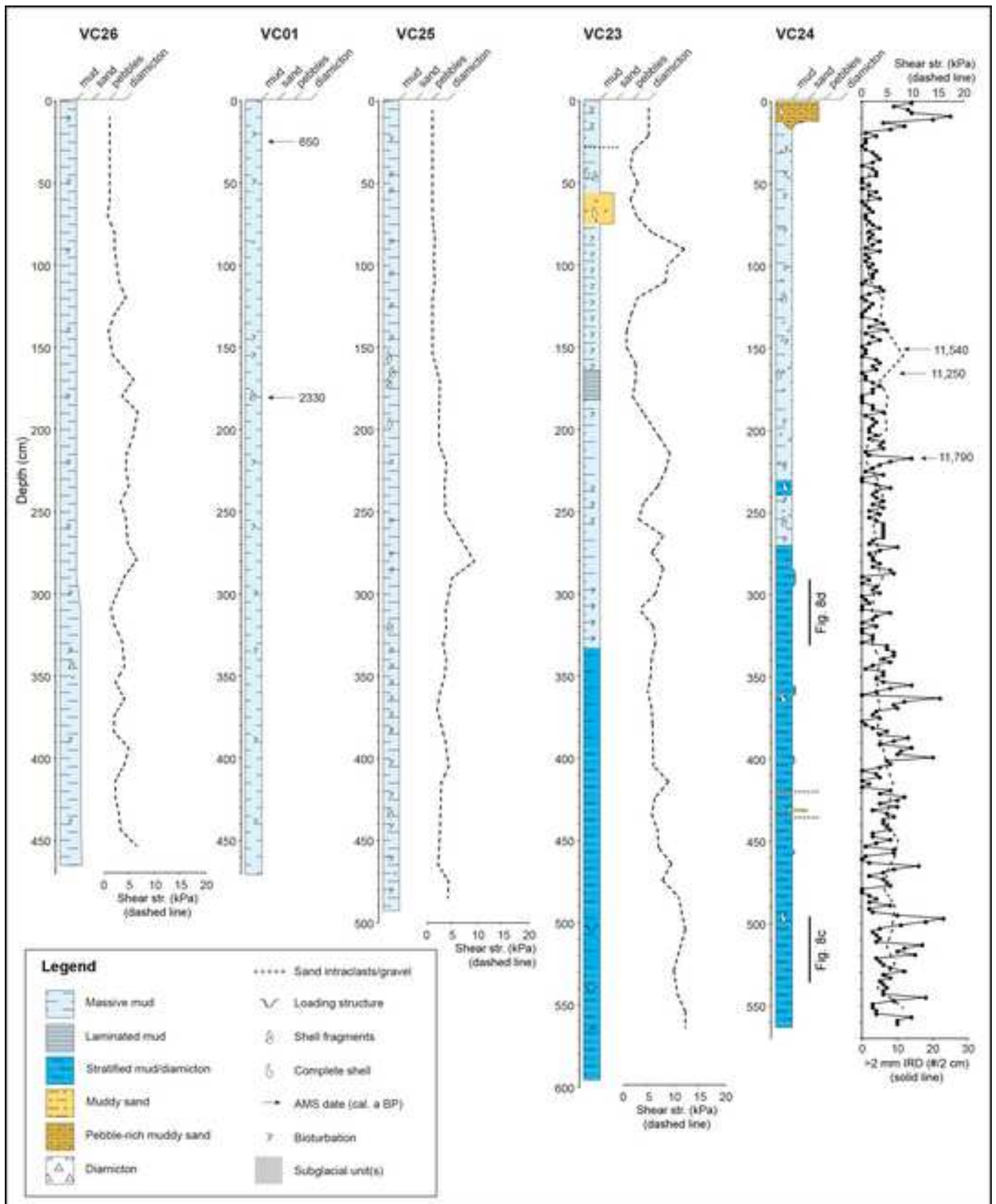


Figure
[Click here to download high resolution image](#)

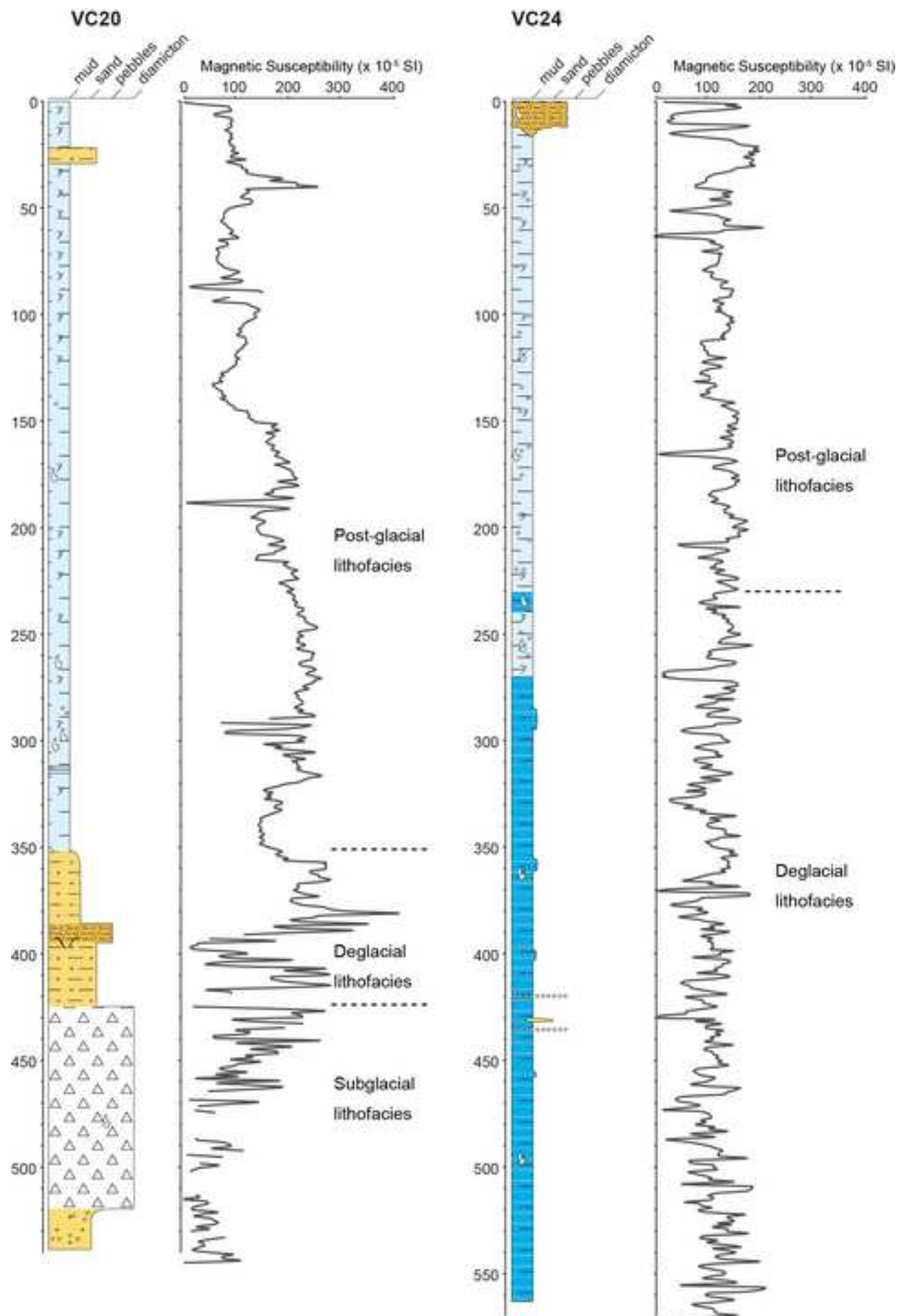


Figure
[Click here to download high resolution image](#)

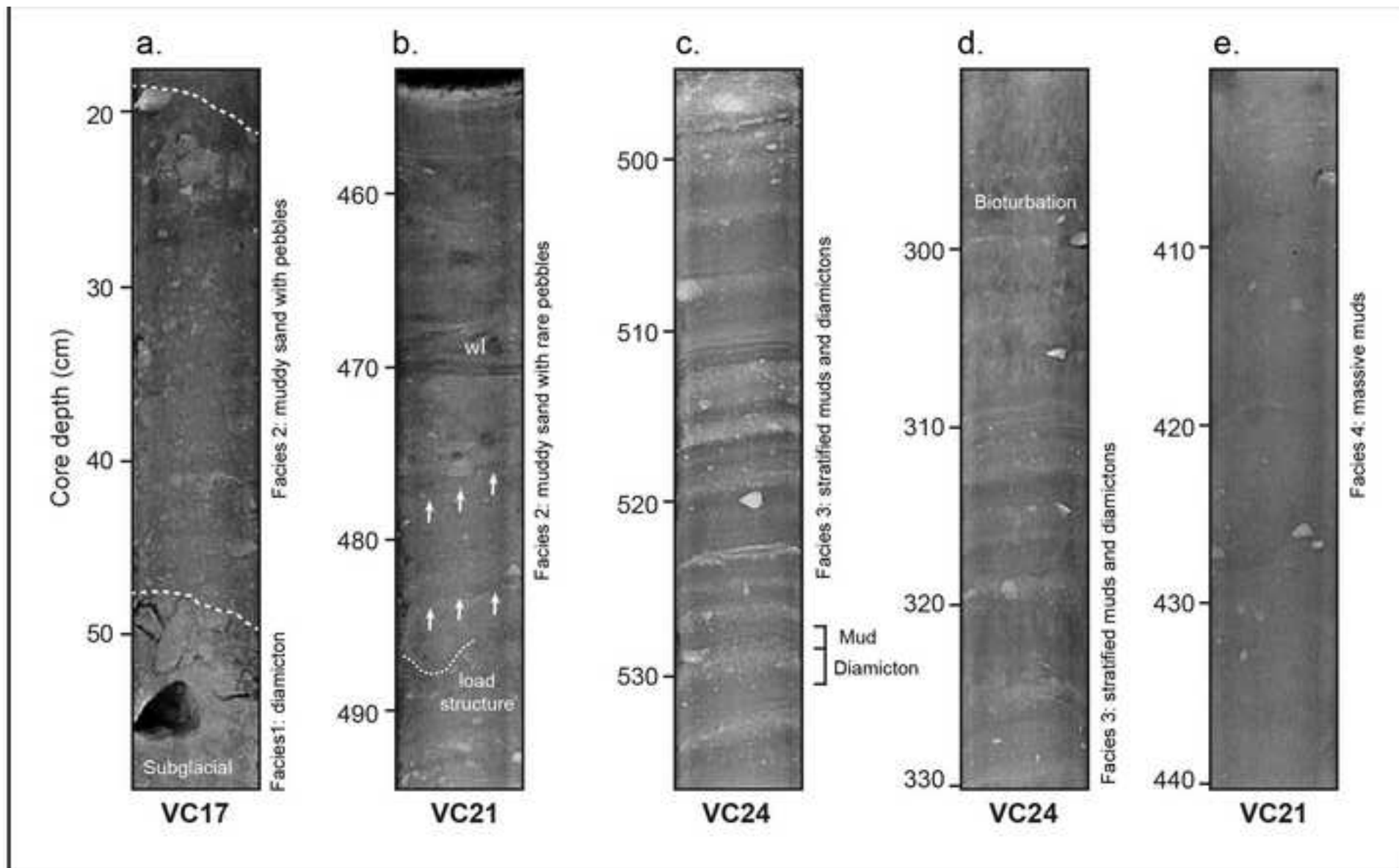


Figure 9
[Click here to download high resolution image](#)

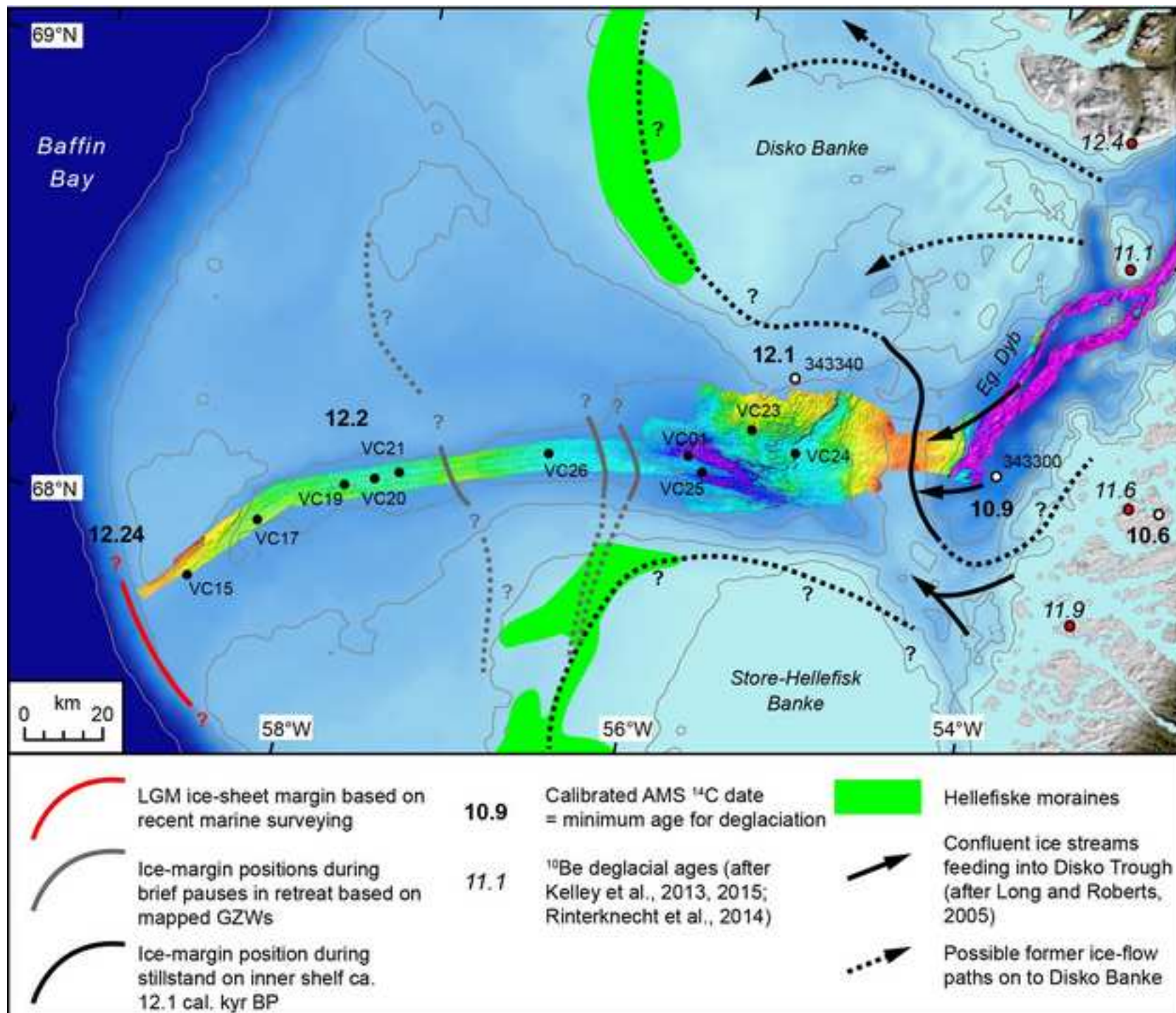


Figure
[Click here to download high resolution image](#)

